

Deformations of Lifshitz Holography in $(n + 1)$ -dimensions

Miok Park ^a and Robert B. Mann ^{a,b}

^a*Department of Physics,
University of Waterloo,
Waterloo, Ontario N2L 3G1,
Canada*

^b*Perimeter Institute for Theoretical Physics,
31 Caroline Street North,
Waterloo, Ontario N2L 2Y5,
Canada*

m7park@uwaterloo.ca, rbmann@uwaterloo.ca

Abstract

We investigate deformations of Lifshitz holography in $(n + 1)$ dimensional spacetime. After discussing the situation for general Lifshitz scaling symmetry parameter z , we consider $z = n - 1$ and the associated marginally relevant operators. These operators are dynamically generated by a momentum scale $\Lambda \sim 0$ and correspond to slightly deformed Lifshitz spacetimes via a holographic picture. We obtain renormalization group flow at finite temperature from UV Lifshitz to IR AdS, and evaluate how physical quantities such as the free energy density and the energy density depend on $\log(\Lambda^z/T)$ in the quantum critical regime as $\Lambda^z/T \rightarrow 0$.

Contents

1	Introduction	2
2	Einstein Gravity with a Massive Vector fields in $(n + 1)$ dimensional spacetime	3
3	Asymptotic Behaviour	5
4	Holographic Renormalization	7
5	Finite Temperature	10
5.1	Expansion and Physical quantities near horizon	11
5.2	Integrated First law of thermodynamics	12
5.3	Integrating towards the Lifshitz Boundary	13
5.3.1	Matching Λ	13
5.3.2	Matching f_0 , and p_0	15
5.3.3	Energy Density, and Free Energy Density	18
5.4	Exploring the dependence of \mathcal{E} and \mathcal{F} on $\log \Lambda^z/T$	18
6	Summary and Discussion	22

1. Introduction

One of the most innovative ideas in theoretical physics in recent years is the anti-de Sitter spacetime/Conformal Field Theory (AdS/CFT) correspondence[1], which posits an isomorphism between symmetries of a spacetime and those of matter fields – for instance, the conformal group $SO(n, 2)$ of a n -dimensional CFT arises as the group of isometries of AdS_{n+1} . This idea has been extended to a duality between gauge theories and gravitational theories in one larger dimension, yielding a new way to understand physics. The most exciting aspect of this picture is to provide a technique for obtaining a weakly coupled and calculable dual description of strongly coupled matter fields in terms of gravity.

Several years prior to the conception of the AdS/CFT correspondence in high energy physics, investigations on phase transitions of modern materials indicated that a precarious point exists between two stable phases of matter such as superconductors and ferroelectrics or ferromagnets in which the temperature of a system has been driven to absolute zero by the application of some external parameter such as pressure or an applied magnetic field. Unlike classical critical points, where critical fluctuations are limited to a narrow region around the phase transition, at such ‘quantum critical points’, the critical fluctuations are quantum mechanical in nature and exhibit a generalized scale invariance in both time and space. Understanding this puzzling behavior has become a major research effort in condensed matter physics. Such systems exhibit universally distinct characteristics upon fanning out to finite temperatures, and so the effect of quantum criticality is felt without ever reaching absolute zero. A recent attempt to understand quantum critical theory involves extending the AdS/CFT correspondence [2], [3] to condensed matter systems, yielding a considerably broader range of scope for gauge/gravity duality.

The signature scaling property underlying quantum critical theory in $2 + 1$ dimensions is

$$t \rightarrow \lambda^z t, \quad \vec{x} \rightarrow \lambda \vec{x} \quad (1.1)$$

where z is the dynamical critical exponent; $z = 1$ corresponds to conformal invariance, whereas $z \neq 1$ implies an anisotropic scaling invariance. Recently a form of gauge-gravity duality was proposed for $z \neq 1$ [4], in which the geometrical dual is obtained from the (asymptotic) metric

$$ds^2 = l^2 \left(-\frac{dt^2}{r^{2z}} + \frac{dr^2}{r^2} + \frac{dx^2 + dy^2}{r^2} \right) \quad (1.2)$$

which is called Lifshitz spacetime and obviously satisfies

$$t \rightarrow \lambda^z t, \quad r \rightarrow \lambda r, \quad \vec{x} \rightarrow \lambda \vec{x}. \quad (1.3)$$

When $z = 1$ the metric (1.2) is that of (asymptotic) AdS spacetime and (1.1) recovers the conformal symmetry of the CFT. When $z = 2$, (1.1) restores the scaling symmetry of quantum critical theories. The more general anisotropic scaling symmetry, $z \neq 1$, submerged in the gravity theory and the field theory, is the foundation for a Lifshitz spacetime/Quantum Critical Theory (Lifshitz/QCT) correspondence.

One issue associated with this approach is how to obtain non-trivial spacetimes that asymptote to the anisotropic metric (1.2). Two approaches have been considered to this end. First, it is obvious from the Einstein equations that an anisotropic energy-momentum tensor could support an anisotropic geometry; for example a massive vector field with the appropriate asymptotic behaviour can suffice. An alternate approach involves adding higher curvature terms into the Einstein action [5]; by appropriately tuning the different gravitational constants, metrics asymptotic to (1.2) can be obtained. In this paper, we follow the first approach, investigating the Einstein action coupled to a massive vector field in $(n + 1)$ dimensions.

Related to Lifshitz field theory, an interesting feature attracting much recent attention is associated with renormalization group flow. The action for the Lifshitz field is

$$S_{Lif} = \frac{1}{2} \int d\tau d^2x \left((\partial_\tau \phi)^2 - \kappa (\nabla^2 \phi)^2 \right), \quad (1.4)$$

where it is clear that the anisotropic scaling invariance has $z = 2$. By perturbing this action with a term $-(\nabla\phi)^2$, Lorentz invariance is recovered in a nontrivial way via renormalization group flow, with the perturbation playing the role of a relevant operator.

In this paper, we consider $(n+1)$ -dimensional Lifshitz spacetime and $((n-1)+1)$ -dimensional Quantum Critical Theory(QCT), and study their holographic duality. While QCT is well described in a $2 + 1$ dimensional context, more general theories of physics including the standard model and gravity are implemented in a higher-dimensional context. The success of the AdS/CFT correspondence therefore provides motivation to understand the extent to which the broader notions of Lifshitz/QCT duality are applicable in higher dimensions, and what different behaviour emerges. Motivated by these interests, we especially focus on the marginally relevant operators in the QCT extended to higher dimensions, with the goal of understanding their behaviour from the perspective of holographic duality, where these operators correspond to the deformed Lifshitz spacetime solutions.

Previous work in this subject has concentrated on the $(2+1)$ -dimensional case [6]. Here we demonstrate that renormalization group flow from Lifshitz spacetime in the UV to AdS spacetime in the IR generalizes to any dimensionality in the marginally relevant case yielding deformations of the pure Lifshitz spacetime. From a thermodynamic perspective, we find that physical quantities such as the ratios s/T (entropy density to temperature), \mathcal{F}/Ts (free energy density to Ts), and \mathcal{E}/Ts (energy density over Ts) exhibit progressively weaker dependence on temperature at sub-leading order in $\log(\Lambda^z/T)$ as dimensionality increases. We also find that the maximal flux of the vector field near the horizon grows linearly with increasing dimension.

In section 2, the action, equations of motion, and basic setup are introduced, along with an ansatz for which all constants are fine-tuned and normalized for both Lifshitz and AdS spacetime. In section 3, asymptotic solutions consistent with a marginally relevant operator are derived by bringing in a dynamically generated momentum scale Λ (assumed very small), which deforms Lifshitz spacetime in the high energy regime. In section 4, we carry out holographic renormalization, rendering the action finite by constructing proper counterterms. In section 5, we numerically match our asymptotic near-Lifshitz solutions with black hole solutions near the horizon. We then describe the renormalization group flow, and compute physical quantities such as the entropy density s , the free energy density \mathcal{F} , and the energy density \mathcal{E} for $n = 3, 4, 5, 6, 7$, and 8.

2. Einstein Gravity with a Massive Vector fields in $(n + 1)$ dimensional spacetime

The action for gravity in $(n + 1)$ -dimensional spacetime coupled to a massive vector field is described by

$$S = \int d^{n+1}x \sqrt{-g} \left(\frac{1}{2\kappa_{n+1}^2} [R + 2\tilde{\Lambda}] - \frac{1}{g_v^2} \left[\frac{1}{4} H^2 + \frac{\gamma}{2} B^2 \right] \right) \quad (2.1)$$

where $\kappa_{n+1} = \sqrt{8\pi G_{n+1}}$ in which G_{n+1} is the $(n + 1)$ dimensional gravitational constant, and $H = dB$ and g_v is the $(n+1)$ dimensional coupling constant of the vector field. The equations of the motion are

$$\frac{1}{\kappa_{n+1}^2} \left(R_{\mu\nu} - \frac{1}{2} g_{\mu\nu} R - \tilde{\Lambda} g_{\mu\nu} \right) = \frac{1}{g_v^2} \left(H_{\mu\rho} H_{\nu}^{\rho} - \frac{1}{4} g_{\mu\nu} H^2 \right) + \frac{\gamma}{g_v^2} \left(B_{\mu} B_{\nu} - \frac{1}{2} g_{\mu\nu} B^2 \right), \quad (2.2)$$

and

$$\nabla_{\mu} H^{\mu\nu} - \gamma B^{\nu} = 0 \quad (2.3)$$

where γ is the squared mass of the vector field. For the action to yield solutions asymptotic to those having the scaling symmetry (1.3), we require the spacetime metric

$$ds^2 = l^2 \left(-\frac{dt^2}{r^{2z}} + \frac{dr^2}{r^2} + \frac{dx^2 + dy^2 + \dots}{r^2} \right) \quad (2.4)$$

to be a solution to the field equations, where z is arbitrary. Note that in these coordinates $r \rightarrow 0$ corresponds to the boundary of the spacetime.

The vector potential yielding a stress-energy supporting this metric is given by

$$B = \frac{g_v l}{\kappa_{n+1}} \frac{q}{r^z} dt. \quad (2.5)$$

These ansatz and boundary conditions fine-tune the cosmological constant to be

$$\tilde{\Lambda} = \frac{(z-1)^2 + n(z-2) + n^2}{2l^2}, \quad (2.6)$$

and the squared mass and the charge of the vector field to be

$$\gamma = \frac{(n-1)z}{l^2}, \quad q^2 = \frac{z-1}{z}. \quad (2.7)$$

Regardless of the dimensionality of the spacetime, setting $z = 1$ in (2.4) yields AdS_{n+1} solution

$$ds_{AdS}^2 = a l^2 \left(-\frac{dt^2}{r^2} + \frac{dr^2}{r^2} + \frac{dx^2 + dy^2 + \dots}{r^2} \right) \quad (2.8)$$

where the vector potential vanishes. As the cosmological constant has been already fixed due to the Lifshitz boundary condition we introduce a scaling constant, a , into the AdS metric and adjust its value to be

$$a = \frac{n(n-1)}{(z-1)^2 + n(z-2) + n^2}. \quad (2.9)$$

Once we fix the cosmological constant (2.6) with space dimension n and dynamical critical exponent z , then those values determine the scaling constant for the AdS spacetime metric.

In order to describe the renormalization group flow which involves breaking the anisotropy of the spacetime by running from the UV Lifshitz to the IR AdS, we employ the ansatz

$$ds^2 = l^2 \left(-f(r)dt^2 + \frac{dr^2}{r^2} + p(r)(dx^2 + dy^2 + \dots) \right), \quad (2.10)$$

$$B = \frac{g_v l}{\kappa_{n+1}} h(r) dt \quad (2.11)$$

so for the Lifshitz spacetime

$$\text{Lifshitz : } f = \frac{1}{r^{2z}} \quad p = \frac{1}{r^2}, \quad h = \frac{\sqrt{z-1}}{\sqrt{z}} \frac{1}{r^z}, \quad (2.12)$$

whereas for the AdS_{n+1} spacetime

$$\text{AdS : } f = p = \frac{n}{(3n-4)} r^{-2\sqrt{\frac{3n-4}{n}}}, \quad h = 0. \quad (2.13)$$

With (2.10) and (2.11), the equations of motion yield three independent non-linear ODEs for $\{f(r), p(r), h(r)\}$

$$\begin{aligned} 2\chi + \frac{z(4n-6)h(r)^2}{f(r)} - \frac{r f'(r)}{f(r)} + \frac{r^2 f'(r)^2}{2f(r)^2} - \frac{(3n-5)r^2 f'(r)p'(r)}{2f(r)p(r)} - \frac{(n-2)^2 r^2 p'(r)^2}{2p(r)^2} - \frac{r^2 f''(r)}{f(r)} &= 0, \\ -\frac{2zh(r)^2}{f(r)} - \frac{rp'(r)}{p(r)} + \frac{r^2 f'(r)p'(r)}{2f(r)p(r)} + \frac{r^2 p'(r)^2}{2p(r)^2} - \frac{r^2 p''(r)}{p(r)} &= 0, \\ \chi + \frac{(n-1)zh(r)^2}{f(r)} - \frac{r^2 h'(r)^2}{f(r)} - \frac{(n-1)r^2 f'(r)p'(r)}{2f(r)p(r)} - \frac{(n-2)(n-1)r^2 p'(r)^2}{4p(r)^2} &= 0, \end{aligned} \quad (2.14)$$

where $\chi = (n-1)^2 + (n-2)z + z^2$. We shall rewrite the equations of the motion with the new variables

$$p(r) = e^{\int^r \frac{q(s)}{s} ds}, \quad f(r) = e^{\int^r \frac{m(s)}{s} ds}, \quad h(r) = k(r)\sqrt{f(r)}. \quad (2.15)$$

These variables have the added benefit of turning the second order differential equations into first order and postponing the determination of rescaling ambiguities on f , p , and h .

For further simplification, we introduce a new variable

$$x(r) = \left(4\chi + 4(n-1)zk(r)^2 - 2(n-1)m(r)q(r) - (n-2)(n-1)q(r)^2 \right)^{\frac{1}{2}}. \quad (2.16)$$

Putting (2.15) and (2.16) into (2.14) gives

$$\begin{aligned} rx'(r) &= -2(n-1)zk(r) - \frac{(n-1)}{2}q(r)x(r), \\ rq'(r) &= \frac{\chi}{(n-1)} - zk(r)^2 - \frac{n}{4}q(r)^2 - \frac{1}{4(n-1)}x(r)^2, \\ rk'(r) &= -\frac{\chi}{(n-1)}\frac{k(r)}{q(r)} - \frac{zk(r)^3}{q(r)} + \frac{(n-2)}{4}k(r)q(r) - \frac{x(r)}{2} + \frac{1}{4(n-1)}\frac{k(r)x(r)^2}{q(r)}. \end{aligned} \quad (2.17)$$

In terms of the new variables $k(r)$, $q(r)$, and $x(r)$, Lifshitz spacetime is described by

$$\text{Lifshitz : } q = -2 \quad x = 2\sqrt{z-1}\sqrt{z}, \quad k = \frac{\sqrt{z-1}}{\sqrt{z}}, \quad (2.18)$$

whereas for AdS spacetime

$$\text{AdS : } q = -2\sqrt{\frac{3n-4}{n}}, \quad x = 0, \quad k = 0. \quad (2.19)$$

As we are interested in the special case for which the energy-momentum tensor of the gravitational field and the operator of the vector field become marginally relevant, the above general description is narrowed down to the case satisfying $z = n-1$. In this case (2.6) becomes

$$\tilde{\Lambda} = \frac{(3n-4)(n-1)}{2l^2}. \quad (2.20)$$

Henceforth we deal with only this $z = n-1$ case.

3. Asymptotic Behaviour

We consider the spacetime slightly thermally heated and so slightly deformed from the pure Lifshitz case, restricting our considerations to $z = n-1$ for which the massive vector field becomes marginal. Under

these assumptions, the general form of the solutions near the boundary $r \rightarrow 0$ is

$$k(r) = \frac{\sqrt{z-1}}{\sqrt{z}} \left(1 + \frac{1}{(z-1)^2 \log(r\Lambda)} + \frac{(z-1)(-3z+2(z-1)^3\lambda) + 2(1-3z)\log(-\log(r\Lambda))}{2z(z-1)^4 \log^2(r\Lambda)} + \dots \right) \\ + (r\Lambda)^{2z} \log^2(r\Lambda) \left(\beta \left(1 + \frac{2(3z-1)\log(-\log(r\Lambda))}{z(z-1)^2 \log(r\Lambda)} + \dots \right) + \alpha \left(\frac{1}{\log(r\Lambda)} + \frac{(2z^2-4z+1) - 2(z-1)^4(2z-1)\lambda + 2(6z^2-5z+1)\log(-\log(r\Lambda))}{2z(z-1)^2(2z-1)\log(r\Lambda)} + \dots \right) \right), \quad (3.1)$$

$$q(r) = -2 \left(1 - \frac{1}{(z-1)\log(r\Lambda)} - \frac{z + 2(z-1)^4\lambda - 2(3z-1)\log(-\log(r\Lambda))}{2z(z-1)^3 \log^2(r\Lambda)} + \dots \right) \\ - \frac{2\sqrt{z-1}\sqrt{z}}{2z-1} (r\Lambda)^{2z} \log^2(r\Lambda) \left(\beta \left(1 + \frac{-z(4z^2-7z+2) + 2(2z-1)(3z-1)\log(-\log(r\Lambda))}{z(z-1)^2(2z-1)\log(r\Lambda)} + \dots \right) \right. \\ \left. + \alpha \left(\frac{1}{\log(r\Lambda)} - \frac{(2z^2-4z+1) + 2(z-1)^4\lambda - 2(3z-1)\log(-\log(r\Lambda))}{2z(z-1)^2 \log^2(r\Lambda)} + \dots \right) \right), \quad (3.2)$$

$$x(r) = 2\sqrt{z-1}\sqrt{z} \left(1 + \frac{z}{(z-1)^2 \log(r\Lambda)} + \frac{(z-1)^4\lambda + (1-3z)\log(-\log(r\Lambda))}{(z-1)^4 \log^2(r\Lambda)} + \dots \right) \\ - \frac{2z^2}{2z-1} (r\Lambda)^{2z} \log^2(r\Lambda) \left(\beta \left(1 + \frac{-z(4z^2-5z+1) + 2(6z^2-5z+1)\log(-\log(r\Lambda))}{z(z-1)^2(2z-1)\log(r\Lambda)} + \dots \right) \right. \\ \left. + \alpha \left(\frac{1}{\log(r\Lambda)} - \frac{(2z-1)^2 + 2(z-1)^4\lambda - 2(3z-1)\log(-\log(r\Lambda))}{2z(z-1)^2 \log^2(r\Lambda)} + \dots \right) \right), \quad (3.3)$$

where Λ is a momentum scale, generating a marginally relevant mode, whereas Λ^z is an energy scale with $n = z + 1$ the spatial dimension. As $\Lambda \rightarrow 0$ the solution recovers the pure Lifshitz spacetime. The parameters α and β describe other modes of the solution, and λ is nothing but a gauge choice [6]. We set $\lambda = 0$ for convenience.

As we are interested in the high energy regime, we expand by introducing an arbitrary scale μ and write

$$\log(r\Lambda) = \log(r\mu) - \log \frac{\mu}{\Lambda}. \quad (3.4)$$

In the high energy regime where $\mu \gg \Lambda$ we have

$$\left| \frac{1}{\log \frac{\mu}{\Lambda}} \right|, \quad \left| \frac{\log(r\mu)}{\log \frac{\mu}{\Lambda}} \right| \leq 1. \quad (3.5)$$

Upon expansion, equations (3.1) \sim (3.3) become

$$k(r) = \frac{\sqrt{z-1}}{\sqrt{z}} \left(1 + \frac{1}{(z-1)^2 \log(\frac{\mu}{\Lambda})} - \frac{3z(z-1) + 2z(z-1)^2 \log(r\mu) + 2(3z-1)\log(-\log(\frac{\mu}{\Lambda}))}{2z(z-1)^4 \log^2(\frac{\mu}{\Lambda})} + \dots \right), \quad (3.6)$$

$$q(r) = -2 \left(1 - \frac{1}{(z-1)\log(\frac{\mu}{\Lambda})} + \frac{-z + 2z(z-1)^2 \log(r\mu) + 2(3z-1)\log(-\log(\frac{\mu}{\Lambda}))}{2z(z-1)^3 \log^2(\frac{\mu}{\Lambda})} + \dots \right), \quad (3.7)$$

$$x(r) = 2\sqrt{z-1}\sqrt{z} \left(1 + \frac{z}{(z-1)^2 \log(\frac{\mu}{\Lambda})} - \frac{z(z-1)^2 \log(r\mu) + (3z-1)\log(-\log(\frac{\mu}{\Lambda}))}{(z-1)^4 \log^2(\frac{\mu}{\Lambda})} + \dots \right). \quad (3.8)$$

Using these solutions for $k(r)$, $q(r)$ and $x(r)$, we employ the change of variables (2.15) and (2.16) in reverse to obtain the original form of the solutions

$$f(\rho) = \frac{F_0^2}{(r\Lambda)^{2z}(-\log(r\Lambda))^{\frac{2z}{z-1}}} \left(1 - \frac{(7z-4) + 2(3z-1)\log(-\log(r\Lambda))}{(z-1)^3 \log(r\Lambda)} - \frac{(23z^4 - 142z^3 + 152z^2 - 57z + 6)}{4z(z-1)^6 \log^2(r\Lambda)} \right. \\ \left. + \frac{(3z-1)^2(5z-2)\log(-\log(r\Lambda)) + (3z-1)^3 \log^2(-\log(r\Lambda))}{z(z-1)^6 \log^2(r\Lambda)} + \dots \right) \quad (3.9)$$

$$p(\rho) = \frac{P_0^2(-\log(r\Lambda))^{\frac{2}{z-1}}}{(r\Lambda)^2} \left(1 + \frac{(5z-2) + 2(3z-1)\log(-\log(r\Lambda))}{z(z-1)^3 \log(r\Lambda)} + \frac{(31z^4 - 64z^3 + 106z^2 - 69z + 14)}{4z^2(z-1)^6 \log^2(r\Lambda)} \right. \\ \left. + \frac{(3z^3 + 26z^2 - 21z + 4)\log(-\log(r\Lambda)) + (3z-1)^2(z-3)\log^2(-\log(r\Lambda))}{z^2(z-1)^6 \log^2(r\Lambda)} + \dots \right) \quad (3.10)$$

where F_0 and P_0 are constants. Furthermore, in the high energy regime the same expansion for eq. (3.9)–(3.10) yields

$$f(\rho) = \frac{1}{r^{2z}} \left(1 + \frac{7z-4 + 2z(z-1)^2 \log(r\mu) + 2(3z-1)\log(\log(\frac{\mu}{\Lambda}))}{(z-1)^3 \log(\frac{\mu}{\Lambda})} + \dots \right), \quad (3.11)$$

$$p(\rho) = \frac{1}{r^2} \left(1 - \frac{5z-2 + 2z(z-1)^2 \log(r\mu) + 2(3z-1)\log(\log(\frac{\mu}{\Lambda}))}{z(z-1)^3 \log(\frac{\mu}{\Lambda})} + \dots \right) \quad (3.12)$$

upon rescaling the t and x coordinates to

$$t \rightarrow \frac{\left(\Lambda \log^{\frac{1}{z-1}}(\frac{\mu}{\Lambda}) \right)^z}{F_0} t, \quad x \rightarrow \left(\frac{\Lambda}{\log^{z-1}(\frac{\mu}{\Lambda})} \right)^2 \frac{1}{P_0} x. \quad (3.13)$$

4. Holographic Renormalization

In this section we investigate thermodynamic quantities such as free energy density or energy density at an asymptotic boundary of the deformed Lifshitz spacetime. We begin with the definition of the free energy density

$$F = -T \log \mathcal{Z} = T S_\epsilon(g) \quad (4.1)$$

where S_ϵ and g_* are respectively the Euclidean action and the metric, and \mathcal{Z} is the partition function. Upon carrying out a variation of the on-shell action, boundary terms arise, and to cancel these out a Gibbons-Hawking boundary term is added into the action. After Euclideanization, the action and the metric can be explicitly written as

$$S_\epsilon = \int d^{n+1}x \sqrt{g} \left(\frac{1}{2\kappa_{n+1}^2} [R + 2\tilde{\Lambda}] - \frac{1}{g_v^2} \left[\frac{1}{4} H^2 + \frac{\gamma}{2} B^2 \right] \right) + \frac{1}{\kappa_{n+1}^2} \int d^n x \sqrt{\gamma} K, \quad (4.2)$$

$$ds_\epsilon^2 = l^2 \left(f(r) d\tau^2 + \frac{dr^2}{r^2} + p(r)(dx^2 + dy^2 + \dots) \right), \quad (4.3)$$

where ϵ indicates the Euclidean version of the quantities.

Calculating the free energy density (the free energy per unit $(n-1)$ -dimensional spatial volume), the Einstein-Hilbert action and Gibbon-Hawking term yield

$$\mathcal{F}_{EH} = -\frac{l^{n-1}}{2\kappa_{n+1}^2} \lim_{r \rightarrow 0} r \sqrt{f(r)} p'(r) p(r)^{\frac{n-3}{2}}, \quad (4.4)$$

$$\mathcal{F}_{GH} = \frac{1}{\kappa_{n+1}^2} \lim_{r \rightarrow 0} \sqrt{\gamma} K = \frac{l^{n-1}}{\kappa_{n+1}^2} \lim_{r \rightarrow 0} r \left(\sqrt{f(r)} p(r)^{\frac{n-1}{2}} \right)' \quad (4.5)$$

where γ_{ab} is the induced metric on the boundary and $K_{\mu\nu}$ is the extrinsic curvature defined as $K_{\mu\nu} = \nabla_\mu n_\nu$ in which n_ν is the normal vector on the boundary surface. The free energy is $F = \int d^{n-1}x \mathcal{F}$. However for the marginally relevant modes both (4.4) and (4.5) are divergent as the boundary ($r \rightarrow 0$) is approached. We incorporate boundary counterterms [7, 8, 9, 10] into the action as a remedy for this problem. We construct these counterterms as a power series in $B^2 = B^\mu B_\mu$ [6], so as to satisfy covariance at the boundary, obtaining

$$\mathcal{F}_{CT} = \frac{1}{2l\kappa_{n+1}^2} \lim_{r \rightarrow 0} \sqrt{\gamma} \sum_{j=0}^2 C_j \left(-\frac{\kappa_{n+1}^2}{g_v^2} B^2 - \frac{(z-1)}{z} \right)^j \quad (4.6)$$

$$= \frac{l^{n-1}}{2\kappa_{n+1}^2} \lim_{r \rightarrow 0} \sqrt{f(r)} p(r)^{\frac{n-1}{2}} \sum_{j=0}^2 C_j \left(k(r)^2 - \frac{(z-1)}{z} \right)^j \quad (4.7)$$

where we have used $(B^2 - (z-1)/z)$ instead of B^2 , since these must vanish for the pure Lifshitz case. The coefficients C_j are not constants but rather a series of the logarithmic functions, with at least three needed to eliminate divergences.

The final expression for the free energy density is

$$\begin{aligned} \mathcal{F} &= \mathcal{F}_{EH} + \mathcal{F}_{GH} + \mathcal{F}_{CT} \\ &= \frac{l^{n-1}}{2\kappa_{n+1}^2} \lim_{r \rightarrow 0} \sqrt{f(r)} p(r)^{\frac{n-1}{2}} \left(\frac{(n-2)rp'(r)}{p(r)} + \frac{rf'(r)}{f(r)} + \sum_{j=0}^2 C_j \left(k(r)^2 - \frac{(z-1)}{z} \right)^j \right). \end{aligned} \quad (4.8)$$

To obtain the energy density, we use the definition of the boundary stress tensor to the case in which additional non-vanishing boundary fields are present [11]. From the boundary stress tensor, we obtain the charge via variation of the on-shell action with respect to the boundary fields; this process in our case produces

$$\delta S = \frac{\sqrt{\gamma}}{2} \tau^{ab} \delta \gamma_{ab} + \mathcal{J}^a \delta B_a. \quad (4.9)$$

Here, however we are dealing not with scalar matter fields but with massive vector fields, and so the usual charge defined by

$$Q = - \int d^{n-2}x \sqrt{\sigma} \xi_a k_b \tau^{ab} \quad (4.10)$$

where $\sqrt{\sigma} = \sqrt{\gamma_{xx} \cdots \gamma_{zz}}$ is the spatial volume element, ξ_a is a boundary Killing fields, and k_b is the unit normal vector to the boundary Cauchy surface, is not conserved. The boundary stress tensor τ^{ab} must therefore be redefined so as to fix the matter fields in the boundary. Employing the vielbein frame defined by

$$\gamma_{ab} = \eta_{\hat{a}\hat{b}} e_{\hat{a}}^a e_{\hat{b}}^b, \quad \eta = \text{diag}(\pm 1, 1, 1, \dots) \quad (4.11)$$

where

$$e^{\hat{t}} = e_{\hat{a}}^t dx^a = \sqrt{f} d\tau, \quad e^{\hat{x}_i} = \sqrt{p} dx_i. \quad (4.12)$$

We find that the variation of the free energy density retains its original form, but that τ^{ab} is replaced with \mathcal{T}^{ab} , where

$$\delta S = \sqrt{\gamma} \mathcal{T}_{\hat{a}}^a \delta e_{\hat{a}}^{\hat{a}} + \mathcal{J}^{\hat{a}} \delta B_{\hat{a}}, \quad (4.13)$$

with

$$\mathcal{T}^{ab} = \mathcal{T}_{\hat{a}}^a e^{\hat{b}a}, \quad \mathcal{T}^{ab} = \tau^{ab} + \frac{1}{\sqrt{\gamma}} \mathcal{J}^{(a} B^{b)}. \quad (4.14)$$

The energy density is then given by

$$\mathcal{E} = \sqrt{\gamma} \tau_t^t + \mathcal{J}^t B_t, \quad (4.15)$$

and the pressure is

$$\mathcal{P} = -\sqrt{\gamma} \tau_x^x. \quad (4.16)$$

Computing the distinct components of \mathcal{E} , we find

$$\begin{aligned} \tau^{ab} &= \frac{2}{\sqrt{\gamma}} \frac{\delta S}{\delta \gamma_{ab}} = \frac{1}{\kappa_{n+1}^2} (K \gamma^{ab} - K^{ab}) \\ &+ \frac{1}{2l\kappa_{n+1}^2} \sum_{j=0}^2 C_j \left(\gamma^{ab} \left(-\frac{\kappa_{n+1}^2}{g_v^2} B^2 - \frac{(z-1)}{z} \right)^j + \frac{2j\kappa_{n+1}^2}{g_v^2} B^a B^b \left(-\frac{\kappa_{n+1}^2}{g_v^2} B^2 - \frac{(z-1)}{z} \right)^{j-1} \right), \end{aligned} \quad (4.17)$$

and

$$\begin{aligned} \mathcal{J}^t &= \sqrt{f(r)} \frac{\delta S}{\delta B_t}, \\ &= \frac{l^{n-2}}{g_v \kappa_{n+1}} \lim_{r \rightarrow 0} \sqrt{f(r)} p(r)^{\frac{n-1}{2}} \left(\frac{r(k(r) \sqrt{f(r)})'}{\sqrt{f(r)}} + k(r) \sum_{j=0}^2 j C_j \left(k(r)^2 - \frac{(z-1)}{z} \right)^{j-1} \right), \\ &= \frac{l^{n-2}}{g_v \kappa_{n+1}} \lim_{r \rightarrow 0} \sqrt{f(r)} p(r)^{\frac{n-1}{2}} \left(-\frac{1}{2} x(r) + k(r) \sum_{j=0}^2 j C_j \left(k(r)^2 - \frac{(z-1)}{z} \right)^{j-1} \right), \end{aligned} \quad (4.18)$$

and other component of \mathcal{J}^a become zero. Putting these together into (4.15) yields

$$\mathcal{E} = \frac{l^{n-1}}{2\kappa_{n+1}^2} \lim_{r \rightarrow 0} \sqrt{f(r)} p(r)^{\frac{n-1}{2}} \left(\frac{(n-1) r p'(r)}{p(r)} - x(r) k(r) + \sum_{j=0}^2 C_j \left(k(r)^2 - \frac{(z-1)}{z} \right)^j \right) \quad (4.19)$$

and

$$\mathcal{P} = -\mathcal{F}. \quad (4.20)$$

Imposing finiteness of physical quantities of (4.8), (4.18), and (4.19), the coefficients of the counter terms

are found to be

$$C_0 = 2(2z-1) - \frac{2z^2}{(2z-1)(z-1)^3 \log^2(r\Lambda)} + \frac{(4z^4 + 2z^3 - 3z^2 - 2z + 1)}{(z-1)^5(2z-1)^2 \log^3(r\Lambda)} + \frac{4z(3z-1) \log(-\log(r\Lambda))}{(z-1)^5(2z-1) \log^3(r\Lambda)} + \dots, \quad (4.21)$$

$$C_1 = z + \frac{2z^3}{(2z-1)(z-1)^2 \log(r\Lambda)} - \frac{z(14z^3 - z^2 - 10z + 3) + 4z^2(2z-1)(3z-1) \log(-\log(r\Lambda))}{2(2z-1)^2(z-1)^4 \log^2(r\Lambda)} - \frac{1}{\log^3(r\Lambda)} \left(\frac{z^2(34z^4 - 54z^3 + 72z^2 - 46z + 9) + 8a(2z-1)^2(z-1)^5}{2z(2z-1)^2(z-1)^6} - \frac{(6z^4 + 25z^3 - 45z^2 + 21z - 3) \log(-\log(r\Lambda))}{(2z-1)^2(z-1)^6} - \frac{2z(3z-1)^2 \log^2(-\log(r\Lambda))}{(z-1)^6(2z-1)} \right) + \dots, \quad (4.22)$$

$$C_2 = \frac{z^2(1-3z)}{4(2z-1)(z-1)} + \frac{z^2(15z^2 - 14z + 3)}{4(2z-1)^2(z-1)^3 \log(r\Lambda)} + \frac{a}{\log^2(r\Lambda)} - \frac{z(3z-1)^2(5z-3) \log(-\log(r\Lambda))}{4(2z-1)^2(z-1)^5 \log^2(r\Lambda)} \quad (4.23)$$

where the first two are infinite series in $1/\log(r\Lambda)$ that include powers of $\log(-\log(r\Lambda))$ such that the order of the $\log(-\log(r\Lambda))$ terms do not exceed the order of the $1/\log(r\Lambda)$ terms. It is sufficient for C_2 to retain terms up to second order in $1/\log(r\Lambda)$. Note that there exists an ambiguity a in these expressions. This ambiguity does not affect numerical evaluation of the free energy density and the energy density that we shall later compute, though it does affect $\mathcal{J}^{\hat{r}}$, reflecting the reaction of the system to changes in the boundary Proca field. Our counter term construction (4.21) – (4.23) is minimal; additional terms such as $C_3(B^2 - (z-1)/z)^3$ or $C_4(B^2 - (z-1)/z)^4$ would also yield solutions.

Applying (4.21) – (4.23) into (4.8), (4.18) and (4.19), the physical quantities become

$$\mathcal{F} = \frac{l^{n-1}}{\kappa_{n+1}^2} \frac{\sqrt{z}}{\sqrt{z-1}(2z-1)} \left(z\alpha - \frac{(2z^3 - 2z^2 - 2z + 1)}{(2z-1)(z-1)^4} \beta \right), \quad (4.24)$$

$$\mathcal{E} = -\frac{l^{n-1}}{\kappa_{n+1}^2} \frac{\sqrt{z}}{\sqrt{z-1}(2z-1)} \left(z\alpha + \frac{(2z^3 - 4z^2 + 4z - 1)}{(2z-1)(z-1)^4} \beta \right), \quad (4.25)$$

$$\mathcal{J}^{\hat{t}} = \frac{1}{g_v} \frac{l^{n-2}}{\kappa_{n+1}} \left(\frac{z(20z^5 + 18z^4 - 22z^3 - 23z^2 + 24z - 5)}{2(z-1)^4(2z-1)^3} + \frac{4(z-1)a}{z} \right) \beta. \quad (4.26)$$

Since the pure Lifshitz solution does not depend on α and β , we expect in this case that

$$\mathcal{F} = \mathcal{E} = \mathcal{J}^{\hat{t}} = 0 \quad (4.27)$$

regardless of the dimension of spacetime.

5. Finite Temperature

In this section, we consider the finite temperature theory by expanding the black hole solution near horizon. Our goal is to describe the renormalization group (RG) flow under the marginally relevant modes, and to predict behaviour of physical quantities such as the free energy density \mathcal{F} and the energy density \mathcal{E} near criticality in order to provide a way of understanding the quantum phase transition from one phase to the critical point via the holographic dictionary. For these purposes, the RG flow corresponding to the h_0 -dependent horizon flux is explained by ensuring the RG flow in the zero temperature limit [4] $\Lambda^z/T \rightarrow \infty$ with $\Lambda \sim 0$ fixed. Furthermore \mathcal{F}/Ts and \mathcal{E}/Ts are found as functions of $\log(\Lambda^z/T)$ in the near-Lifshitz spacetime containing the large flux.

5.1 Expansion and Physical quantities near horizon

We assume a black hole solution having the form of (2.10) and defined by $f(r_+) = 0$, and expand the solution near horizon $r = r_+$. In this expansion the unknown coefficients arising in every order in the $f(r)$, $g(r)$ and $h(r)$ are calculated by the equations of the motion (2.15). Regularity requires g_{tt} to have a double zero at the horizon, with g_{xx} remaining nonzero. Under these considerations the functions are expressed by

$$f(r) = f_0 \left(\left(1 - \frac{r}{r_+}\right)^2 + \left(1 - \frac{r}{r_+}\right)^3 + \frac{(-6z^2 + 14z + 7)z + 8(3z - 2)h_0^2}{12z} \left(1 - \frac{r}{r_+}\right)^4 + \dots \right), \quad (5.1)$$

$$p(r) = p_0 \left(1 + \frac{(3z - 1)z - 4h_0^2}{2z} \left(1 - \frac{r}{r_+}\right)^2 + \frac{(3z - 1)z - 4h_0^2}{2z} \left(1 - \frac{r}{r_+}\right)^3 + \dots \right), \quad (5.2)$$

$$h(r) = \sqrt{f_0} \left(h_0 \left(1 - \frac{r}{r_+}\right)^2 + h_0 \left(1 - \frac{r}{r_+}\right)^3 + h_0 \left(\frac{z(-9z^2 + 10z + 20) + 8h_0^2(3z - 1)}{24z} \right) \left(1 - \frac{r}{r_+}\right)^4 + \dots \right) \quad (5.3)$$

where the constants f_0 and p_0 are associated with scaling ambiguities of the coordinates $\{t, x, y, \dots\}$, which function as the clock and rulers of the system. Upon fixing these the only variable left in the metric is h_0 . Different values of h_0 correspond to different black holes and so we have a 1-parameter family of black hole solutions.

Some physical information, for example thermodynamic quantities, can be obtained near the horizon of the black hole. At $r = r_+$, the temperature T , can be computed by identifying the imaginary time coordinate τ with period β so as to ensure regularity of the metric, and the entropy density, s , obtained from the definition of the entropy, $S = \frac{A}{4G_{n+1}}$. We find

$$T = \frac{r_+}{2\pi} \sqrt{\frac{1}{2} \frac{d^2 f(r)}{dr^2}} \Big|_{r=r_+}, \quad (5.4)$$

$$s = 2\pi \frac{l^{n-1}}{\kappa_{n+1}^2} p(r_+)^{\frac{n-1}{2}}, \quad (5.5)$$

where $S = \int s d^{n-1}x$.

The horizon flux, Φ , of the massive vector field is

$$\Phi = \oint \sqrt{h} \vec{E} \cdot d\vec{A} = \oint \phi d^{n-1}x \quad (5.6)$$

where

$$\phi = \frac{l^{n-2} g_v r_+}{\kappa_{n+1}} \left(\frac{p(r)^{\frac{n-1}{2}}}{\sqrt{f(r)}} \frac{dh(r)}{dr} \right) \Big|_{r=r_+} \quad (5.7)$$

is the horizon flux density. Using (5.1)–(5.3) we obtain

$$T = \frac{\sqrt{f_0}}{2\pi}, \quad s = 2\pi p_0^{\frac{n-1}{2}} \frac{l^{n-1}}{\kappa_{n+1}^2}, \quad \phi = 2h_0 p_0^{\frac{n-1}{2}} \left(\frac{l^{n-2} g_v}{\kappa_{n+1}} \right). \quad (5.8)$$

for the temperature, entropy density, and horizon flux density.

5.2 Integrated First law of thermodynamics

Before embarking on our numerical calculations, in this section we obtain relationships between the free energy density and the energy density derived in section 4 and the above thermodynamic quantities. We then use this to obtain analytic predictions when the marginally relevant mode vanishes, i.e. $\Lambda \rightarrow 0$.

First, by using the asymptotic solutions (3.1) – (3.3) we construct an r -independent RG-invariant quantity

$$\begin{aligned}\bar{K} &= -\frac{1}{2}\sqrt{f(r)}p(r)^{\frac{n-1}{2}}\left(-q(r) + m(r) + k(r)x(r)\right), \\ &= -\frac{\sqrt{f(r)}p(r)^{\frac{n-1}{2}}}{4(n-1)q(r)}\left(4\chi + 4(n-1)zk(r)^2 - n(n-1)q(r)^2 - x(r)^2 + 2(n-1)q(r)k(r)x(r)\right),\end{aligned}\quad (5.9)$$

where plugging (3.6)–(3.8) into the above gives

$$\bar{K} = \frac{2\sqrt{z}}{\sqrt{z-1}(1-2z)}\left(z\alpha - \frac{(z^2-3z+1)}{(1-2z)(z-1)^2}\beta\right). \quad (5.10)$$

Near the horizon, this RG-invariant quantity can be calculated by using (5.1) – (5.3) and expressed in terms of T and s by applying (5.8). We find

$$\bar{K} = \sqrt{f_0}p_0^{\frac{n-1}{2}} = Ts\frac{\kappa_{n+1}^2}{l^{n-1}}. \quad (5.11)$$

Next, from the free energy density (4.8) and the energy density (4.19) we obtain the following relation

$$\begin{aligned}&\frac{1}{2}\sqrt{f(r)}p(r)^{\frac{n-1}{2}}\left(\frac{(n-1)rp'(r)}{p(r)} - x(r)k(r) + \sum_{j=0}^2 C_j\left(k(r)^2 - \frac{(z-1)}{z}\right)^j\right) \\ &= \frac{1}{2}\sqrt{f(r)}p(r)^{\frac{n-1}{2}}\left(\frac{(n-2)rp'(r)}{p(r)} + \frac{rf'(r)}{f(r)} + \sum_{j=0}^2 C_j\left(k(r)^2 - \frac{(z-1)}{z}\right)^j\right) + \bar{K},\end{aligned}\quad (5.12)$$

which is more simply expressed as

$$\mathcal{E} = \mathcal{F} + \frac{l^{n-1}}{\kappa_{n+1}^2}\bar{K}. \quad (5.13)$$

This relation is easily checked using (4.24), (4.25) and (5.11).

Finally, combining (5.11) with (5.13) gives

$$\mathcal{F} = \mathcal{E} - Ts. \quad (5.14)$$

which is the integrated form of the first law for these black holes. We will use this to check the accuracy of our numerical results in section 5.4.

Considering the limit $\Lambda = 0$, since anisotropic scale invariance still holds, from the Ward identity we expect that the pressure is equal to the energy [12]. From (4.20), we have

$$\mathcal{F}_0 = -\mathcal{E}_0 \quad (\Lambda = 0), \quad (5.15)$$

and in conjunction with (5.14), we obtain an analytic prediction for when the marginally relevant modes are not excited

$$\mathcal{F}_0 = -\mathcal{E}_0 = -\frac{1}{2}Ts_0 \quad (\Lambda = 0), \quad (5.16)$$

which will be used for a consistency check on our numerical results in section 5.4. Note that the relation $\mathcal{F} = -\mathcal{E}$ also holds for $\Lambda \sim 0$ case when $\beta = 0$, as is easily seen from equations (4.24) and (4.25).

5.3 Integrating towards the Lifshitz Boundary

To investigate Lifshitz spacetime in the UV-region, $T \gg \Lambda^z$, we re-expand the asymptotic solutions into the high energy regime by using (3.5), and set the arbitrary scale $\mu \sim r_+^{-1}$, thereby making the marginally relevant modes near-Lifshitz. Upon carrying this out, the deformed Lifshitz spacetime is described in the high temperature regime with fixed $\Lambda \sim 0$. This spacetime approaches a pure-Lifshitz by supplying heat at much greater temperatures or higher energy scales. This process of expansion yields a constant $\log(\Lambda r_+)$ which must be fixed in the asymptotic regions. Near the horizon the expanded black hole solution has three parameters f_0 , p_0 , and h_0 where f_0 and p_0 will be determined, depending on which asymptotic spacetime is imposed.

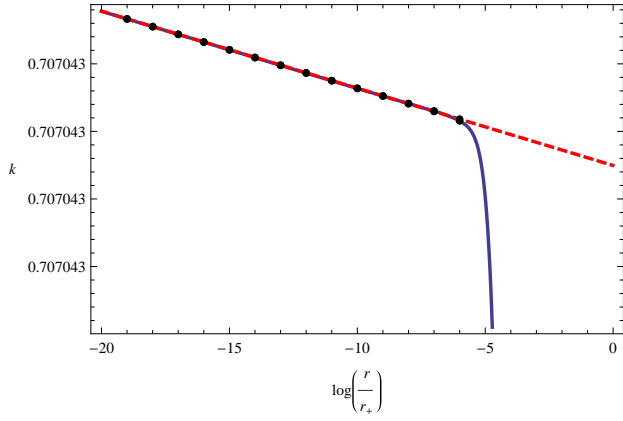
In this section, we numerically connect the expanded near-horizon black hole solution with the near-Lifshitz asymptotic solution. By matching two solutions, we determine the constant $\log(\Lambda r_+)$ which corresponds to h_0 in section 5.3.1, and f_0 and p_0 in section 5.3.2. Then with these values we compute the thermodynamic quantities, varying the value of h_0 . We compute the entropy density as a function of $\log(\Lambda^z/T)$ in section 5.3.2, and the free energy density and energy density versus $\log(r/r_+)$ in section 5.3.3. In section 5.4, we compute the free energy density and energy density as functions of $\log(\Lambda^z/T)$ and find a suitable fitting curve, obtaining a prediction on the sub-leading order of the free energy and energy density as a function of $\log(\Lambda^z/T)$. We also discuss how renormalization group flow is described in our context in section 5.3.1. In our numerical work, we use r/r_+ as our radial variable, and unitless quantities such as \mathcal{F}/Ts , \mathcal{E}/Ts , and Λ^z/T are considered.

5.3.1 Matching Λ

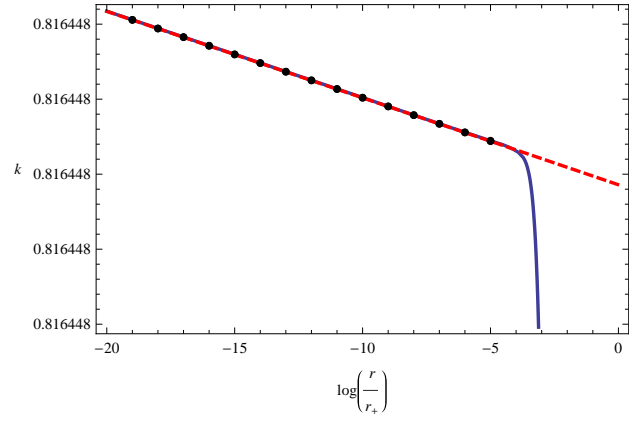
For extracting Λ , we start with the asymptotic solutions $k(r)$, $q(r)$, and $x(r)$ in (3.1) – (3.3). As the UV-deformation is applicable to Lifshitz spacetime in the high energy limit $\Lambda^z/T \rightarrow 0$, we expand the solutions as in (3.6) – (3.8), bringing in the arbitrary scale $\mu \gg \Lambda$ eventually setting $\mu \rightarrow r_+^{-1}$. Then, near the asymptotic boundary, we have only to fix the variable $\log(\Lambda r_+)$. Near the horizon, the expanded black hole solutions (5.1)–(5.3) transfer to functions of $k(r)$, $q(r)$, and $x(r)$ by (2.15) and (2.16), and in this process f_0 and p_0 drop out and h_0 only remains. Now, having a proper value of h_0 , we numerically integrate from the near horizon to the boundary satisfying the equations of motion (2.17), matching the numerical solutions to the asymptotic expectation by adjusting the value of $\log(\Lambda r_+)$ in the middle region. In our numerical works, the integration starts at $\log(r/r_+) \sim -0.015$ and ends at $\log(r/r_+) \sim -10^4$. Our numerical results for the k function are shown in figure 1, where the red dashed line is a fit for the asymptotic expectation and the blue solid line corresponds to the numerical results. We note that the agreement between our numerical results and the asymptotic expectations is very strong.

The important outcome of this procedure is that a maximum value of h_0 is obtained. In other words, if we keep increasing the value of h_0 then beyond a certain point we are not able to find a matching condition connecting our numerical result to the asymptotic expectation. Physically this means that at a large value of flux, the metric functions grow exponentially as the boundary is approached, so they do not ever reach the boundary. This means that under the condition of large flux and high temperature $\Lambda^z/T \rightarrow 0$, the spacetime having the black hole (5.1)–(5.3) is no longer deformed, but rather is asymptotic to pure Lifshitz spacetime. We also find that the maximum values of h_0 linearly increased according to the critical exponent, z (or the spatial dimension) of the spacetime, n . We present this behaviour in Figure 2, and explicitly denote the maximum values of h_0 in Table 1.

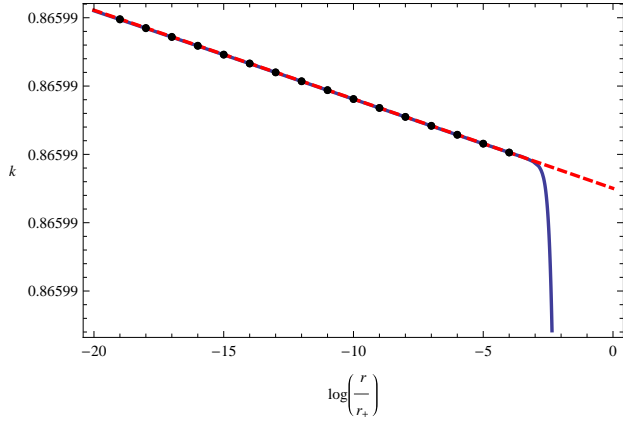
On the other hand, a minimum value of the flux also exists and its value becomes zero at the horizon. In this case, the massive vector field disappears and the spacetime is described by an asymptotically AdS black hole. Examining the situation for h_0 between h_{max} and h_{min} is non-trivial. However for a small amount of flux we can verify that in the zero temperature limit $\Lambda^z/T \rightarrow \infty$ the renormalization group flow



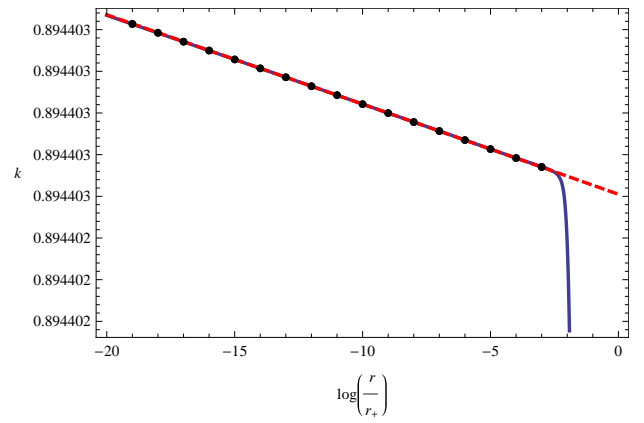
(a) $z = 2$ and $h_0 = 0.97128$, $\log(\Lambda r_+) = -11141.7$



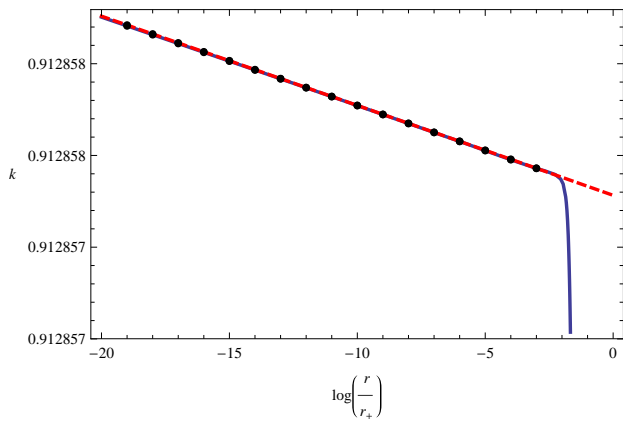
(b) $z = 3$ and $h_0 = 1.63428$, $\log(\Lambda r_+) = -4188.2$



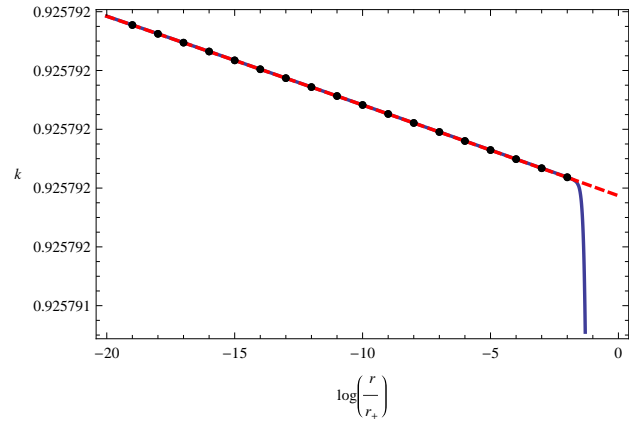
(c) $z = 4$ and $h_0 = 2.28218$, $\log(\Lambda r_+) = -2709.4$



(d) $z = 5$ and $h_0 = 2.92548$, $\log(\Lambda r_+) = -2270.6$



(e) $z = 6$ and $h_0 = 3.56678$, $\log(\Lambda r_+) = -2726$



(f) $z = 7$ and $h_0 = 4.20680$, $\log(\Lambda r_+) = -908.7$

Figure 1: Extracting $\log(\Lambda r_+)$

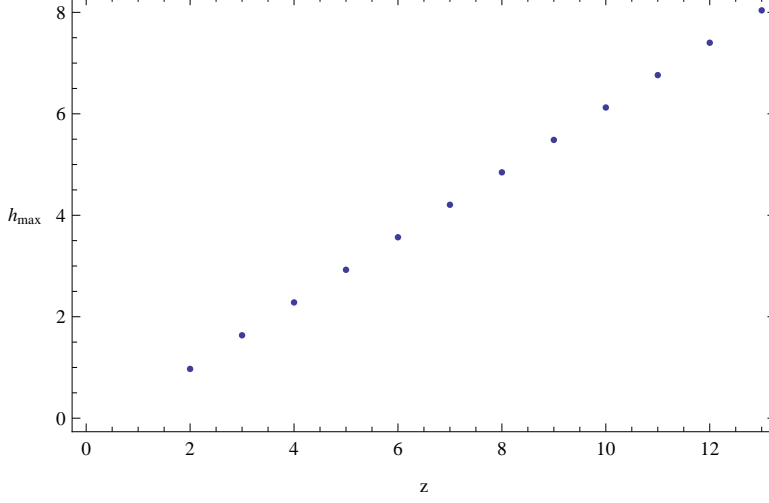


Figure 2: h_{max} versus z

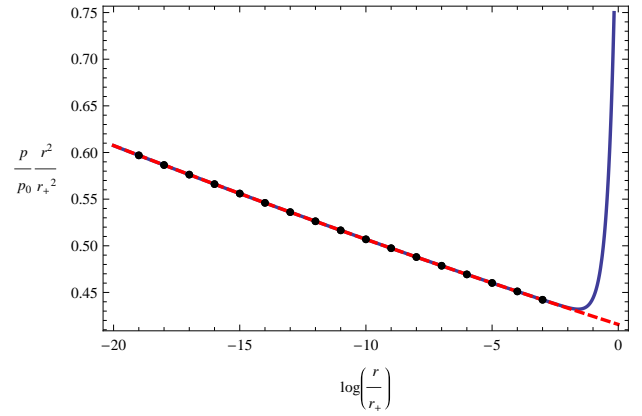
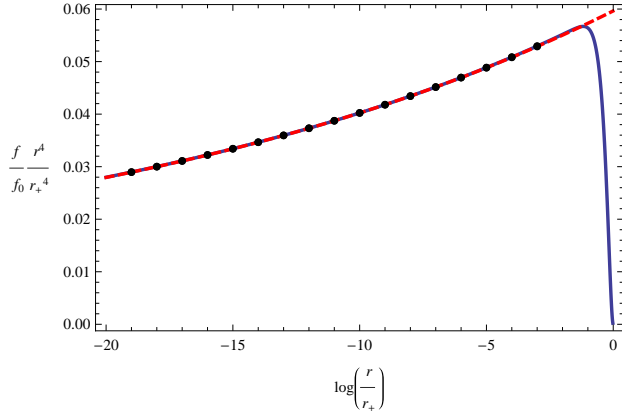
is recovered [4]. This obviously indicates the existence of an RG flow with the marginally relevant mode, and also implies that tuning the horizon flux via h_0 interpolates between the zero temperature RG flow [4] and asymptotic Lifshitz black holes [7, 12, 13, 14, 15, 16].

5.3.2 Matching f_0 , and p_0

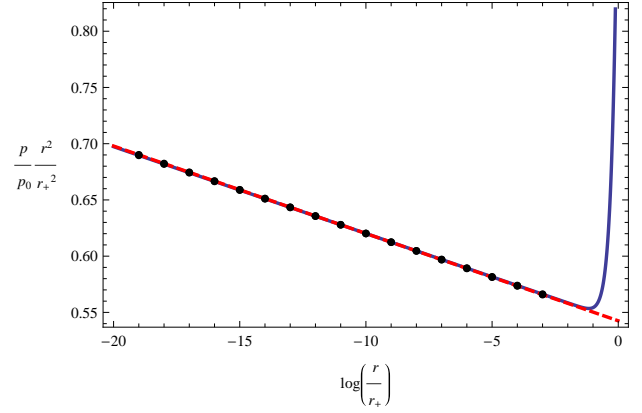
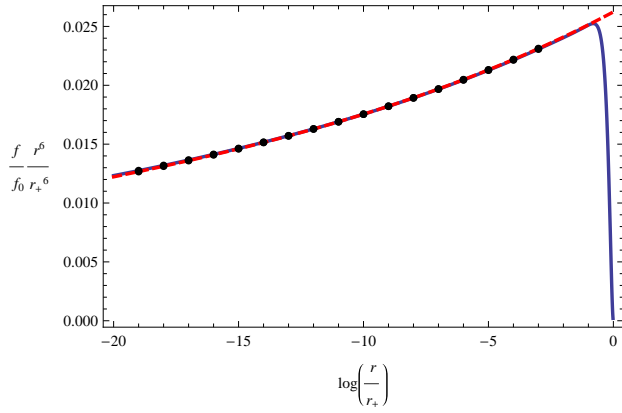
Since, given h_0 , $\log(\Lambda r_+)$ is fixed, f_0 and p_0 arising in (5.1) – (5.3) can be determined. Repeating the previous process with the functions of f , p , and h , the asymptotic solutions (3.9) – (3.10) are in the high energy regime obtained via the expansion of (3.5) and the rescaling of (3.13), becoming the expressions (3.11)–(3.12). We can neglect the α and β involved in the exponent terms because these contribute much

	h_{max}
$z = 2$	0.9713
$z = 3$	1.6343
$z = 4$	2.2822
$z = 5$	2.9255
$z = 6$	3.5668
$z = 7$	4.2070
$z = 8$	4.8465
$z = 9$	5.4856
$z = 10$	6.1244
$z = 11$	6.7629
$z = 12$	7.4012
$z = 13$	8.0394
\vdots	\vdots

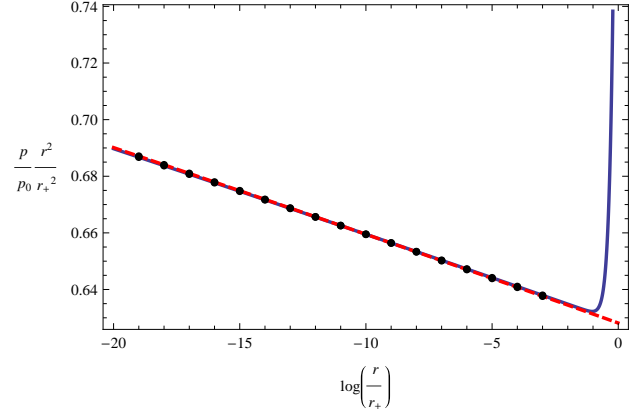
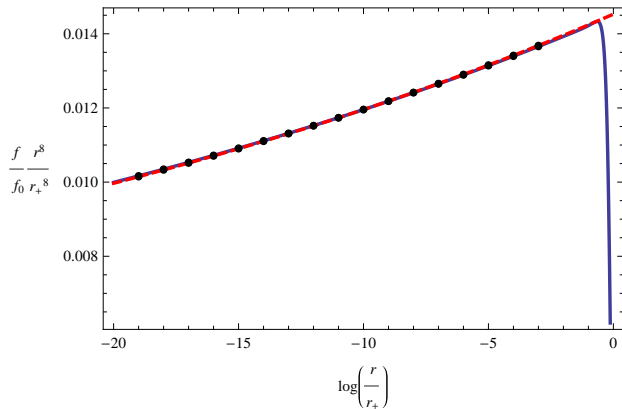
Table 1: maximum value of h_0



(a) For $z = 2$ and $h_0 = 0.962$, which corresponds to $\log(\Lambda r_+) = -106.8$, the red dashed line is matched to the blue solid line at $f_0 r_+^4 = 29.04$ (left) and at $p_0 r_+^2 = 1.8428$ (right).

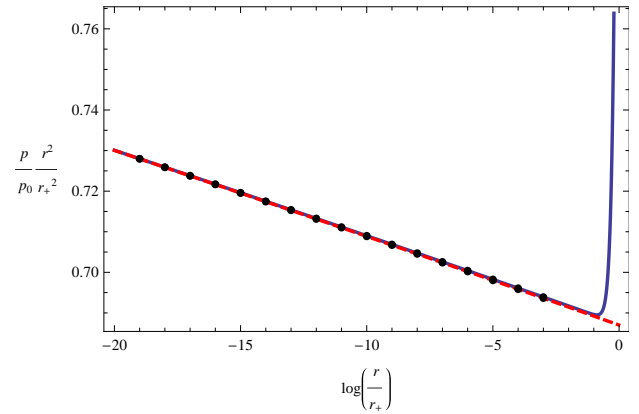
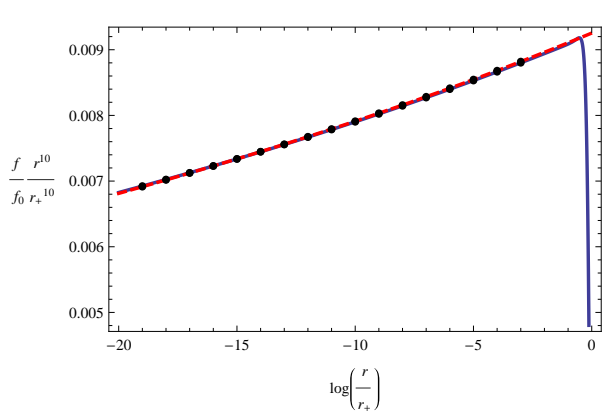


(b) For $z = 3$ and $h_0 = 1.628$, which corresponds to $\log(\Lambda r_+) = -72.6$, the red dashed line is matched to the blue solid line at $f_0 r_+^6 = 44.266$ (left) and at $p_0 r_+^2 = 1.7579$ (right).

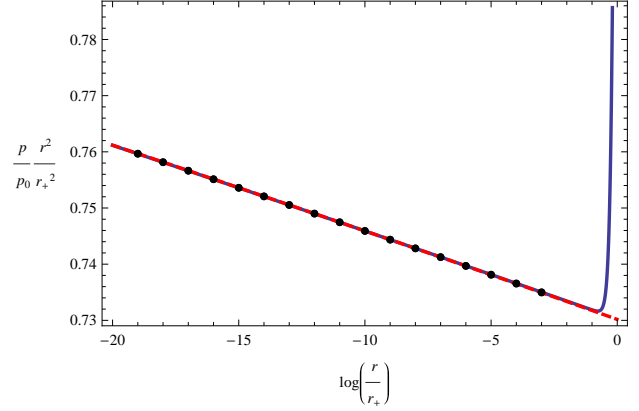
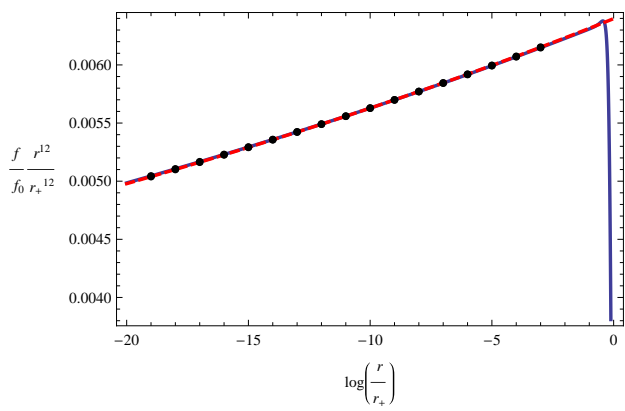


(c) For $z = 4$ and $h_0 = 2.2798$, which corresponds to $\log(\Lambda r_+) = -133.4$, the red dashed line is matched to the blue solid line at $f_0 r_+^8 = 71.40$ (left) and at $p_0 r_+^2 = 1.5781$ (right).

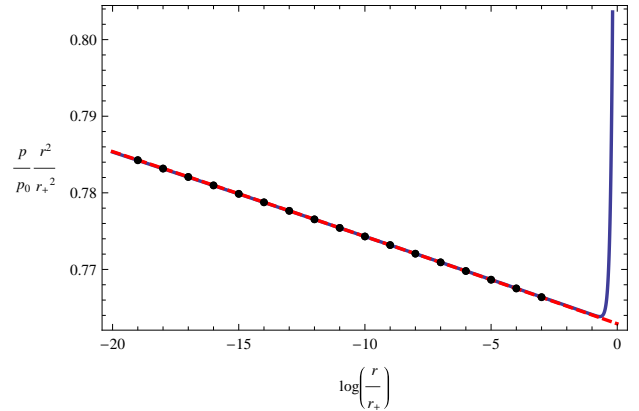
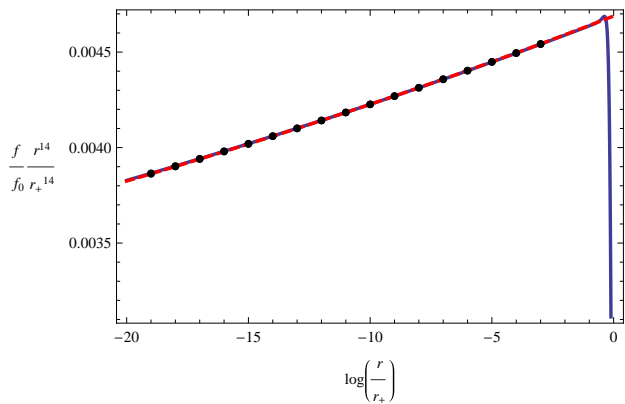
Figure 3: Extracting f_0 and p_0 for $z = 2, 3$, and 4



(a) For $z = 5$ and $h_0 = 2.9238$, which corresponds to $\log(\Lambda r_+) = -155.6$, the red dashed line is matched to the blue solid line at $f_0 r_+^{10} = 109.953$ (left) and at $p_0 r_+^2 = 1.45079$ (right).



(b) For $z = 6$ and $h_0 = 3.5655$, which corresponds to $\log(\Lambda r_+) = -183$, the red dashed line is matched to the blue solid line at $f_0 r_+^{12} = 157.777$ (left) and at $p_0 r_+^2 = 1.36751$ (right).



(c) For $z = 7$ and $h_0 = 4.206$, which corresponds to $\log(\Lambda r_+) = -220.2$, the red dashed line is matched to the blue solid line at $f_0 r_+^{14} = 214.442$ (left) and at $p_0 r_+^2 = 1.3098$ (right).

Figure 4: Extracting f_0 and p_0 for $z = 5, 6$, and 7

less than the logarithmic terms as the boundary is approached (technically these unknowns are hard to fix). Applying the same numerical technique, we start to integrate from the near horizon towards the boundary governed by the equation of motion (2.14). Over a finite range, provided values of h_0 and $\log(\Lambda r_+)$, the numerical solutions and asymptotic expectations (3.11)–(3.12) are matched by finding values of $f_0 r_+^{2z}$ and $p_0 r_+^2$. Our numerical calculations are carried out over a range of 4 to 9 dimensional spacetime. The results are shown in figures 3 and 4 where the red dashed line is a plot of the asymptotic expectation and the blue solid line is the numerical result.

Using the fixed constants Λ , f_0 , and p_0 we next explore physical quantities of interest. Computing the entropy density, derived in (5.8) and determined by $f_0 r_+^{2z}$ and $p_0 r_+^2$, we plot s/T as a function of $\log(\Lambda^z/T)$ in figure 5. Here, the value of $\log(\Lambda^z/T)$, equivalent to $\log(\Lambda r_+)$, is obtained from the relation between the thermodynamic variables in (5.8), which is

$$\log\left(\frac{\Lambda^z}{T}\right) = z \log(\Lambda r_+) + \log(2\pi) - \frac{1}{2} \log(f_0 r_+^{2z}). \quad (5.17)$$

We explicitly consider dimensionalities ranging from 4 to 9.

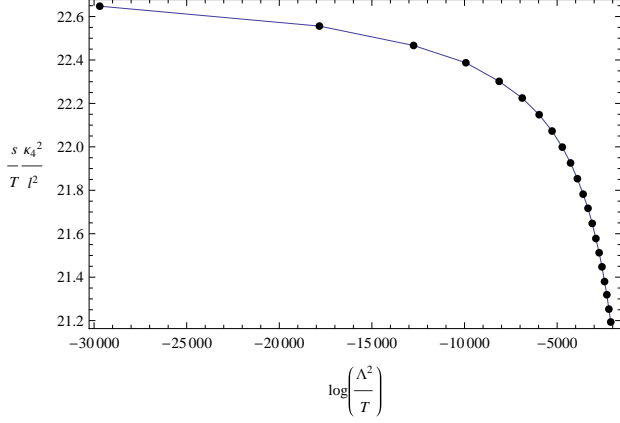
5.3.3 Energy Density, and Free Energy Density

Now we move to the free energy density (4.8) and energy density (4.19). Putting the numerical results of k , q , and x functions into (4.8) by using (2.15) and (2.16), and applying the counterterm (4.21) – (4.23), the free energy density and the energy density are respectively depicted in figures 6 and 7. We find that the free energy density and the energy density have a flat region over some finite range of $\log(r/r_+)$, yield a stable constant value for these quantities. In these figures we also illustrate oscillating and divergent behaviours as the boundary is approached. Recall that initially the physical quantities having marginally relevant modes diverge at the boundary, necessitating the addition of counterterms to render them finite. The counterterms should be expanded in an infinite series in $\log(\Lambda r)$. However in practice the counterterms (4.21) – (4.23) are truncated at a finite order, while our numerical results include higher orders than ones we considered in the analytic calculation. This limitation is responsible for the unstable behavior near the boundary that appears in figure 6 and 7.

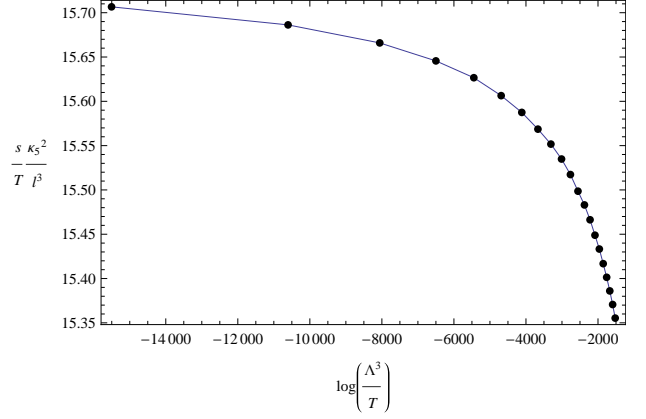
As the spacetime dimension increases we find that the flat region gets narrower and the divergence behaviour starts more quickly from the horizon. The main reason for this is due to the $\sqrt{f} p^{z/2}$ factor commonly appearing in the free energy density (4.8) and the energy density (4.19); both \sqrt{f} and $p^{z/2}$ vary as $1/r^z$ (as shown in (3.12)) as the boundary $r \rightarrow 0$ is approached, whereas the quantities in the parentheses of (4.8) and (4.19) contain no divergent terms.

5.4 Exploring the dependence of \mathcal{E} and \mathcal{F} on $\log \Lambda^z/T$

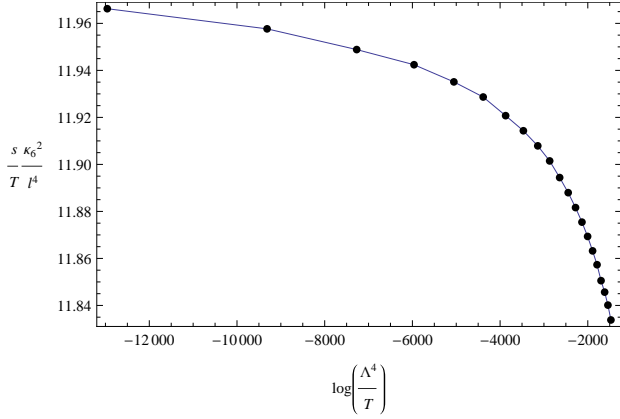
In this section, we numerically compute the free energy density per Ts (\mathcal{F}/Ts), and the energy density per Ts (\mathcal{E}/Ts), as functions of $\log(\Lambda^z/T)$, and investigate their behaviour in terms of T , assuming that Λ is very small and fixed. Figure 8 and 9 present our results for these quantities and for \mathcal{F}/\mathcal{E} . We also include the fitting function depicted as a solid line. As expected from analytic considerations for the leading order terms of \mathcal{F}/Ts and \mathcal{E}/Ts from (5.14) for $\Lambda = 0$, we recover from our numerical results the same value for the leading order terms. In addition, as the marginally relevant modes generated by $\Lambda \sim 0$ are numerically evaluated, their effect is also shown in Figure 8 and 9. Their behaviour predicts the sub-leading terms expressed as functions of $\log(\Lambda^z/T)$. For each z , the fitting functions of \mathcal{F}/Ts , \mathcal{E}/Ts , and \mathcal{F}/\mathcal{E} are presented in Table 2.



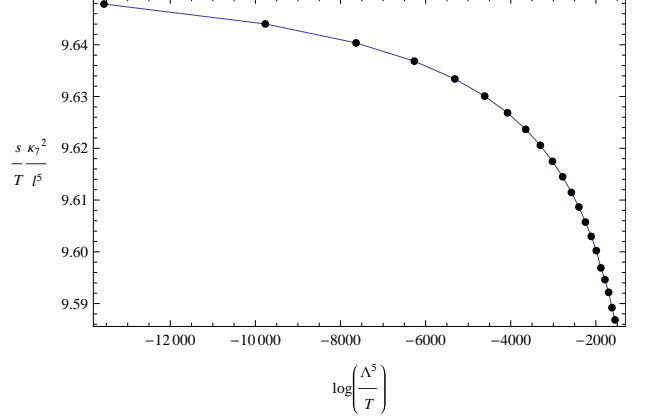
(a) Dots are calculated under that $z = 2$ and h_0 runs from 0.9713 to 0.9705 in increments of 0.00004 and are joined by straight lines.



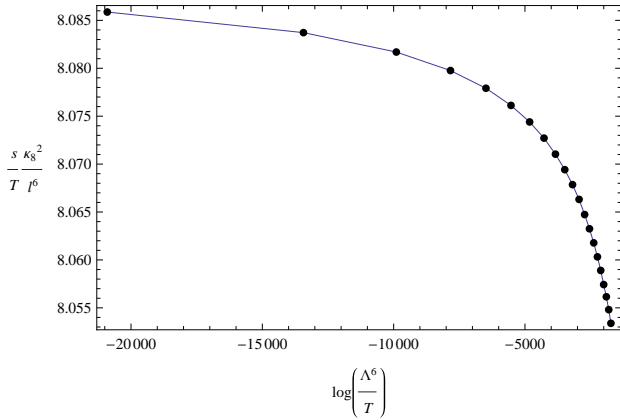
(b) Dots are calculated under that $z = 3$ and h_0 runs from 1.6343 to 1.6335 in increments of 0.00004 and are joined by straight lines.



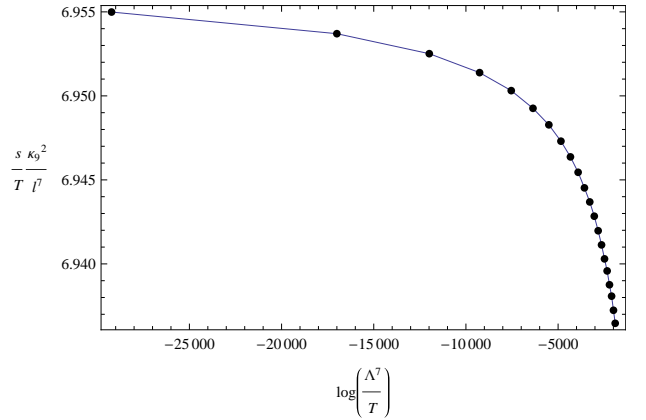
(c) Dots are calculated under that $z = 4$ and h_0 runs from 2.2822 to 2.2814 in increments of 0.00004 and are joined by straight lines.



(d) Dots are calculated under that $z = 5$ and h_0 runs from 2.9255 to 2.9247 in increments of 0.00004 and are joined by straight lines.

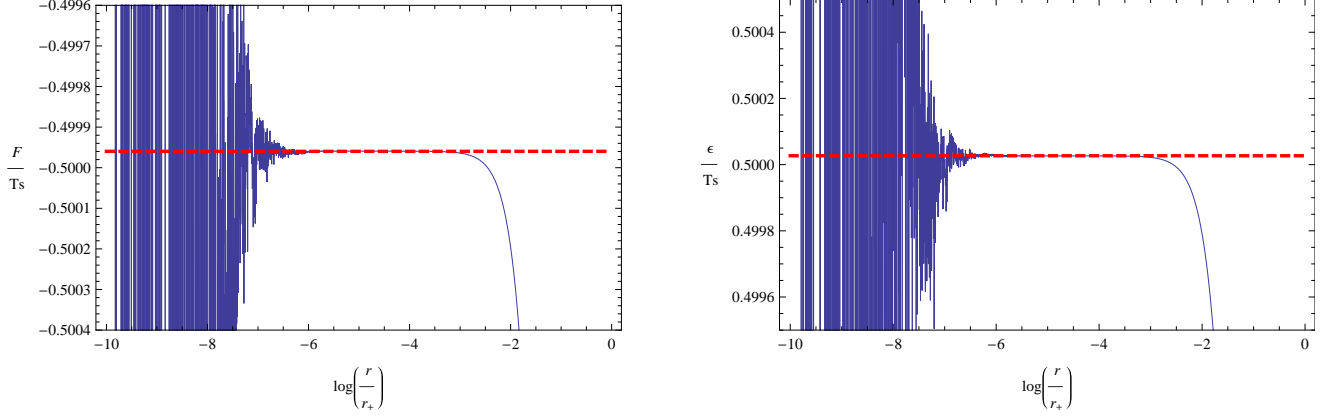


(e) Dots are calculated under that $z = 6$ and h_0 runs from 3.5668 to 3.566 in increments of 0.00004 and are joined by straight lines.

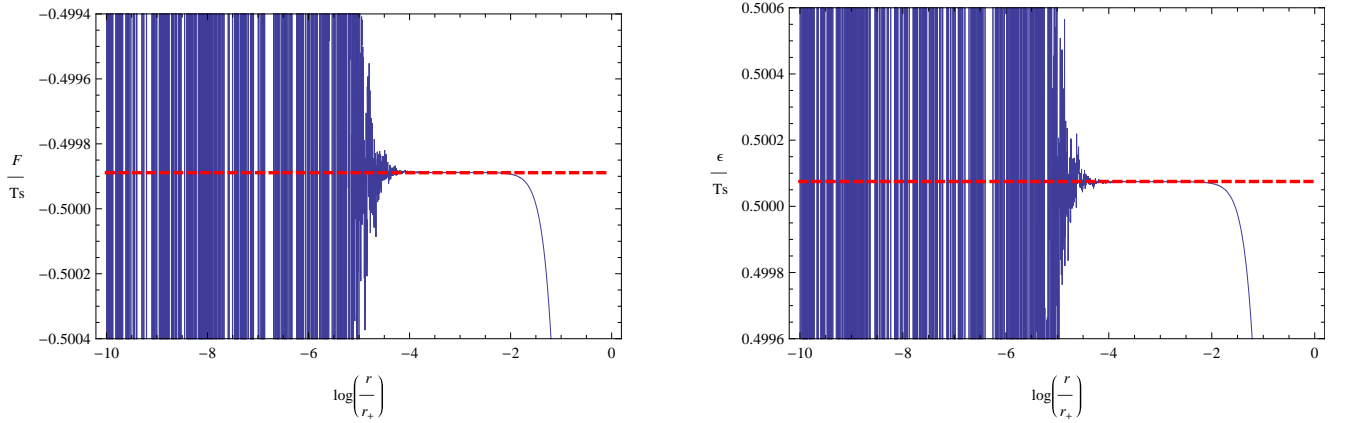


(f) Dots are calculated under that $z = 7$ and h_0 runs from 4.2070 to 4.2062 in increments of 0.00004 and are joined by straight lines.

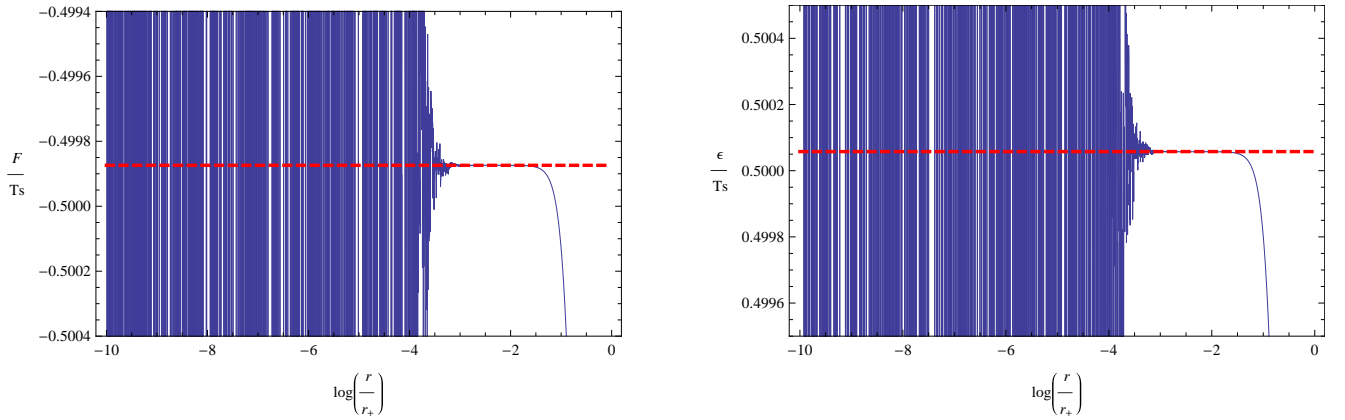
Figure 5: Entropy density per unit temperature versus $\log(\Lambda^z/T)$



(a) When $z = 2$ and $h_0 = 0.97102$, corresponding to $\log(\Lambda^2/T) \sim -5270$, the left is the numerical result of free energy density \mathcal{F} over Ts and the right is the numerical result of energy density \mathcal{E} over Ts , as a function of $\log(r/r_+)$. The quantity is well defined in the intermediate region. Red dashed line is reading-off the constant value of \mathcal{F}/Ts in the intermediate regime.

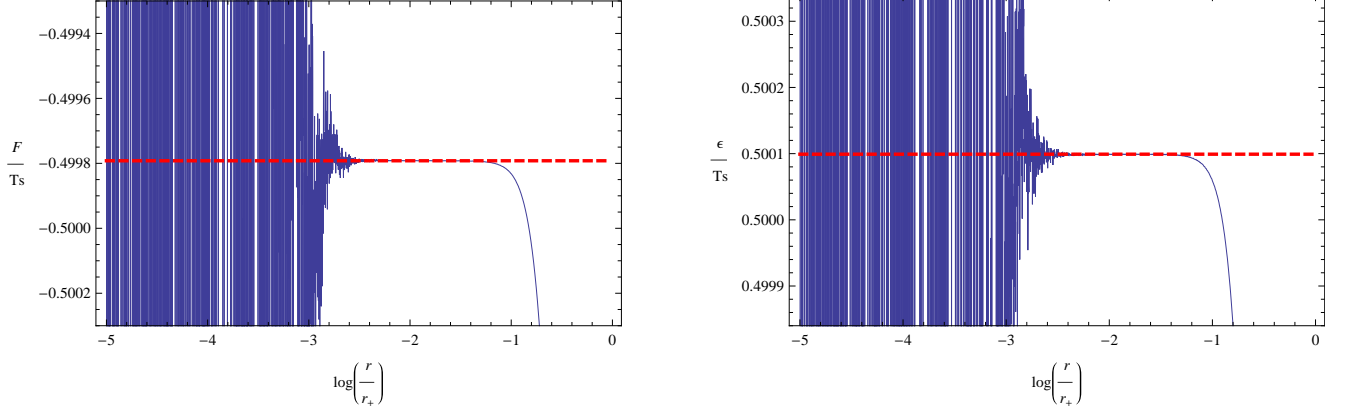


(b) When $z = 3$ and $h_0 = 1.63422$, corresponding to $\log(\Lambda^2/T) \sim -8000$, the left is the numerical result of free energy density \mathcal{F} over Ts and the right is the numerical result of energy density \mathcal{E} over Ts , as a function of $\log(r/r_+)$. The quantity is well defined in the intermediate region. Red dashed line is reading-off the constant value of \mathcal{F}/Ts in the intermediate regime.

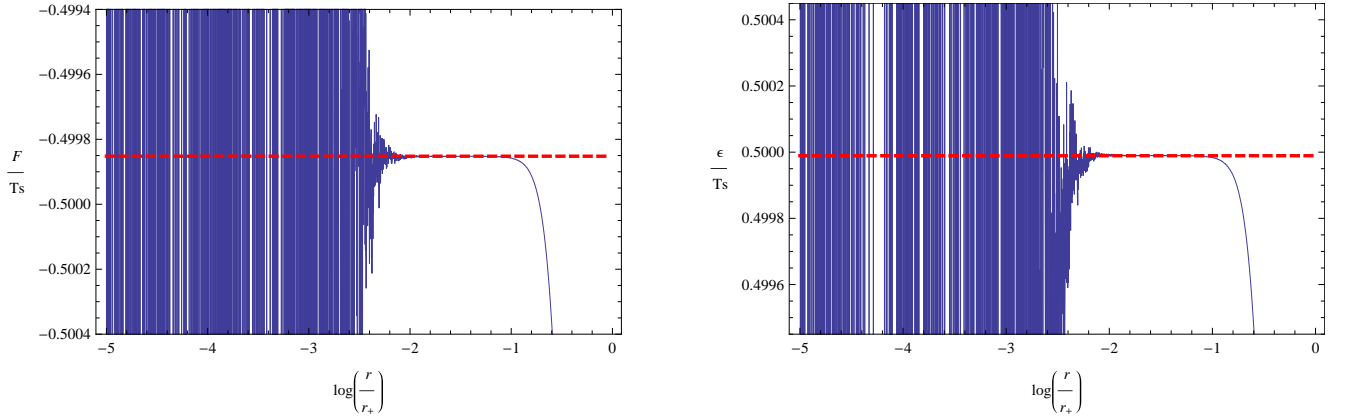


(c) When $z = 4$ and $h_0 = 2.28212$, corresponding to $\log(\Lambda^2/T) \sim -7000$, the left is the numerical result of free energy density \mathcal{F} over Ts and the right is the numerical result of energy density \mathcal{E} over Ts , as a function of $\log(r/r_+)$. The quantity is well defined in the intermediate region. Red dashed line is reading-off the constant value of \mathcal{F}/Ts in the intermediate regime.

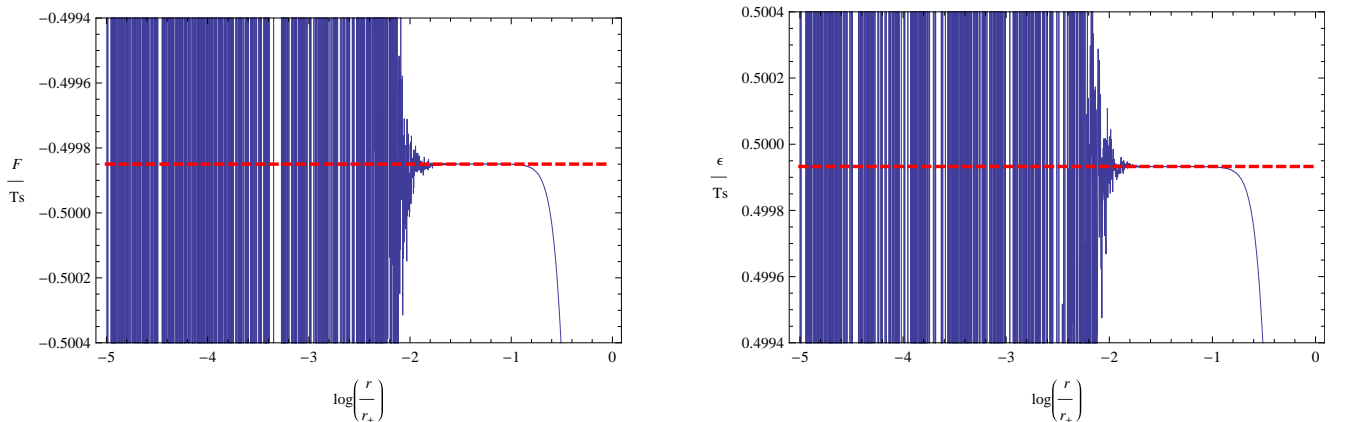
Figure 6: \mathcal{F}/Ts and \mathcal{E}/Ts versus $\log(\frac{r}{r_+})$ for $z = 2, 3$, and 4



(a) When $z = 5$ and $h_0 = 2.92526$, corresponding to $\log(\Lambda^2/T) \sim -4100$, the left is the numerical result of free energy density \mathcal{F} over Ts and the right is the numerical result of energy density \mathcal{E} over Ts , as a function of $\log(r/r_+)$. The quantity is well defined in the intermediate region. Red dashed line is reading-off the constant value of \mathcal{F}/Ts in the intermediate regime.



(b) When $z = 6$ and $h_0 = 3.56670$, corresponding to $\log(\Lambda^2/T) \sim -8700$, the left is the numerical result of free energy density \mathcal{F} over Ts and the right is the numerical result of energy density \mathcal{E} over Ts , as a function of $\log(r/r_+)$. The quantity is well defined in the intermediate region. Red dashed line is reading-off the constant value of \mathcal{F}/Ts in the intermediate regime.



(c) When $z = 7$ and $h_0 = 4.20694$, corresponding to $\log(\Lambda^2/T) \sim -14000$, the left is the numerical result of free energy density \mathcal{F} over Ts and the right is the numerical result of energy density \mathcal{E} over Ts , as a function of $\log(r/r_+)$. The quantity is well defined in the intermediate region. Red dashed line is reading-off the constant value of \mathcal{F}/Ts in the intermediate regime.

Figure 7: \mathcal{F}/Ts and \mathcal{E}/Ts versus $\log(\frac{r}{r_+})$ for $z = 5, 6$, and 7

In addition, the marginally relevant mode should be consistent with the first law of black hole thermodynamics, which is $-\mathcal{F}/Ts + \mathcal{E}/Ts - 1 = 0$. We plot this in figure 10 as a check on the accuracy on our numerical results. We find that our numerical errors are found between the order of 10^{-3} and 10^{-4} .

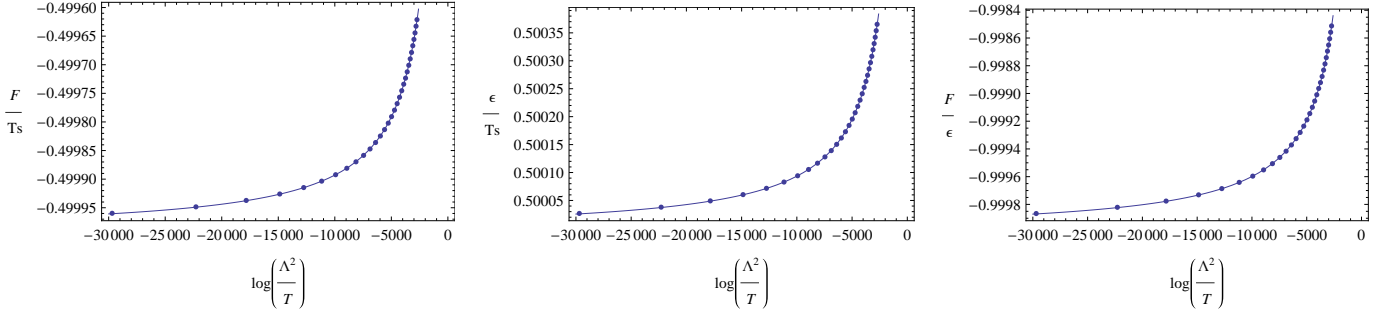
	free energy density over Ts ($\frac{\mathcal{F}}{Ts} =$)	energy density over Ts ($\frac{\mathcal{E}}{Ts} =$)	free energy density over energy density ($\frac{\mathcal{F}}{\mathcal{E}} =$)
$z = 2$	$-\frac{1}{2} - \frac{1}{\log \Lambda^2/T} + \dots$	$\frac{1}{2} - \frac{1}{\log \Lambda^2/T} + \dots$	$-1 - \frac{4}{\log \Lambda^2/T} + \dots$
$z = 3$	$-\frac{1}{2} - \frac{0.76}{\log \Lambda^3/T} + \dots$	$\frac{1}{2} - \frac{0.76}{\log \Lambda^3/T} + \dots$	$-1 - \frac{3}{\log \Lambda^3/T} + \dots$
$z = 4$	$-\frac{1}{2} - \frac{0.67}{\log \Lambda^4/T} + \dots$	$\frac{1}{2} - \frac{0.67}{\log \Lambda^4/T} + \dots$	$-1 - \frac{2.7}{\log \Lambda^4/T} + \dots$
$z = 5$	$-\frac{1}{2} - \frac{0.63}{\log \Lambda^5/T} + \dots$	$\frac{1}{2} - \frac{0.63}{\log \Lambda^5/T} + \dots$	$-1 - \frac{2.50}{\log \Lambda^5/T} + \dots$
$z = 6$	$-\frac{1}{2} - \frac{0.60}{\log \Lambda^6/T} + \dots$	$\frac{1}{2} - \frac{0.60}{\log \Lambda^6/T} + \dots$	$-1 - \frac{2.40}{\log \Lambda^6/T} + \dots$
$z = 7$	$-\frac{1}{2} - \frac{0.58}{\log \Lambda^7/T} + \dots$	$\frac{1}{2} - \frac{0.58}{\log \Lambda^7/T} + \dots$	$-1 - \frac{2.33}{\log \Lambda^7/T} + \dots$
\vdots	\vdots	\vdots	\vdots

Table 2: fitting functions for $\frac{\mathcal{F}}{Ts}$, $\frac{\mathcal{E}}{Ts}$, and $\frac{\mathcal{F}}{\mathcal{E}}$

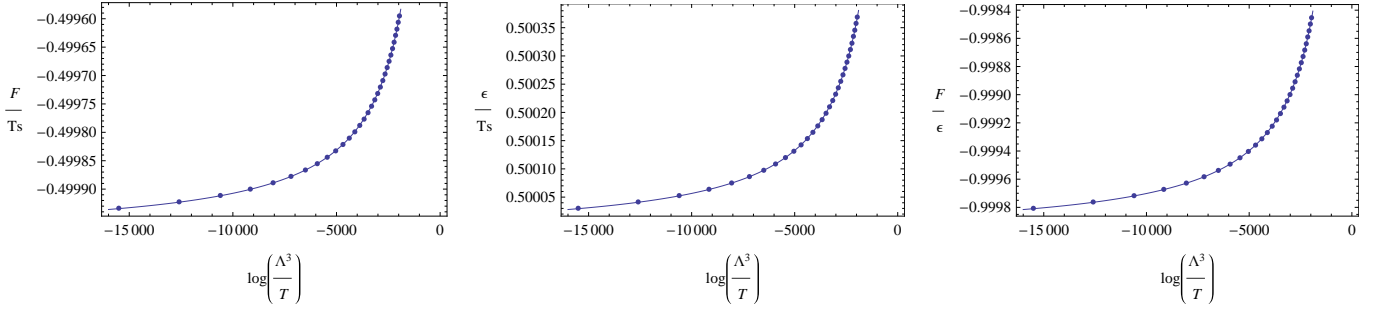
6. Summary and Discussion

We have carried out a study of the deformations of Lifshitz spacetime in higher-dimensions, where the deformation is produced by the marginally relevant modes due to $\Lambda \sim 0$, which is the dynamically generated scale. Our main objective was to describe the renormalization group flow of the marginally relevant operators and to investigate the thermodynamic behaviour at finite temperatures in terms of the dimensionality of the spacetime. We began with the assumption [4] that the deformation is small in the UV-region and leads to renormalization group flow into IR-region, where the Lifshitz spacetime is described in the high temperature limit $\Lambda^z/T \rightarrow 0$ and the AdS spacetime is formed in the zero temperature limit $\Lambda^z/T \rightarrow \infty$.

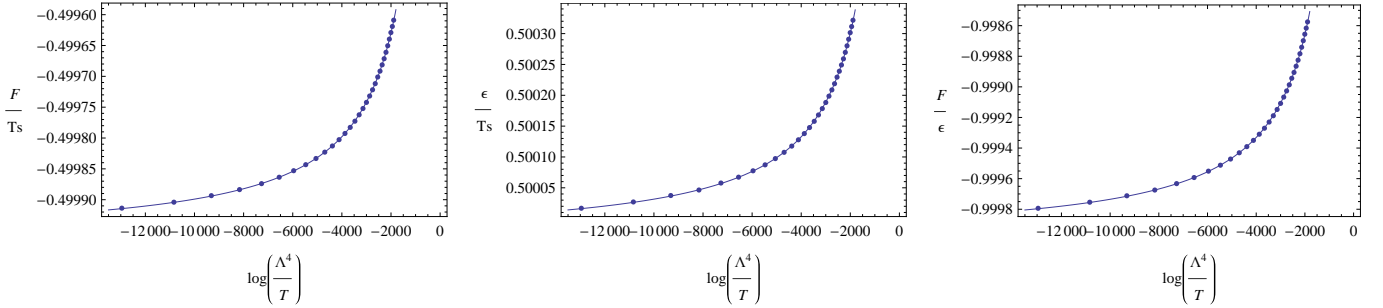
We derived the equation of motion for Einstein gravity with the massive vector field, and set up the ansatz for the metric and the vector potential for both Lifshitz spacetime and AdS spacetime in section 2. In section 3, we obtained asymptotic solutions in terms of functions k , q , and x and also in functions of f , p , and h (used separately for later numerical work), and derived the free energy density \mathcal{F} and the energy density \mathcal{E} at the spacetime boundary in section 4. Since the marginally relevant modes make the action and the physical quantities diverge, we performed holographic renormalization by adding counterterms, constructed from the covariant quantity $(k^2 - (z-1)/z)$. The coefficients C_j in the counterterm expansion were obtained as a series in $\log(\Lambda r_+)$. We also obtained near-horizon expansions of (planar) black hole solutions in section 5.1, and proved that our analytical results are consistent with the first law of the black hole thermodynamics as $\Lambda = 0$, which means the marginally relevant modes are turned off. Numerically we computed in space-time dimensions 4 to 9 the entropy density s/T , the free energy density \mathcal{F}/Ts , and the energy density \mathcal{E}/Ts as functions of $\log(\Lambda^z/T)$ in near-Lifshitz spacetime.



(a) Plots of \mathcal{F}/Ts , \mathcal{E}/Ts , and \mathcal{F}/\mathcal{E} , as a function of $\log(\Lambda^2/T)$ for $z = 2$. Dots are numerical results running h_0 from 0.9713 to 0.9707, which corresponds to $\log(\Lambda^2/T)$ from about -30000 to -2700. Solid line is fitting equations in table 1.

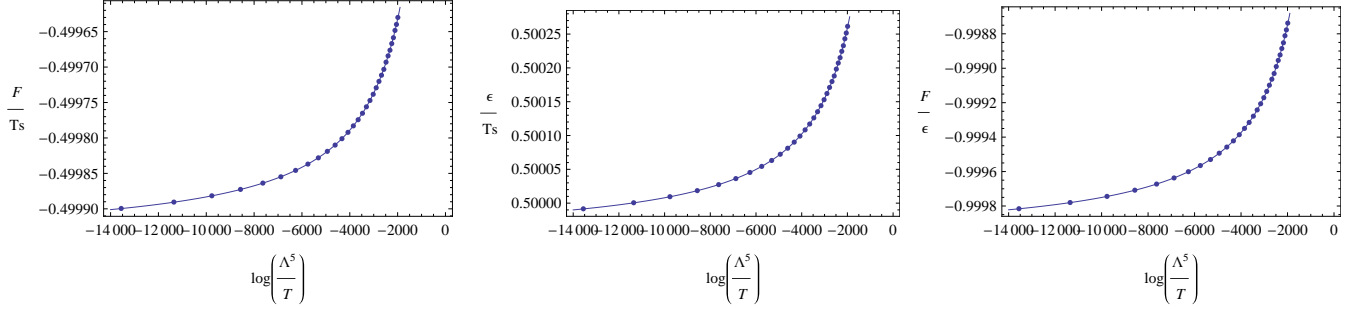


(b) Plots of \mathcal{F}/Ts , \mathcal{E}/Ts , and \mathcal{F}/\mathcal{E} , as a function of $\log(\Lambda^3/T)$ for $z = 3$. Dots are numerical results running h_0 from 1.6343 to 1.6337, which corresponds to $\log(\Lambda^3/T)$ from about -15500 to -2000. Solid line is fitting equations in table 1.

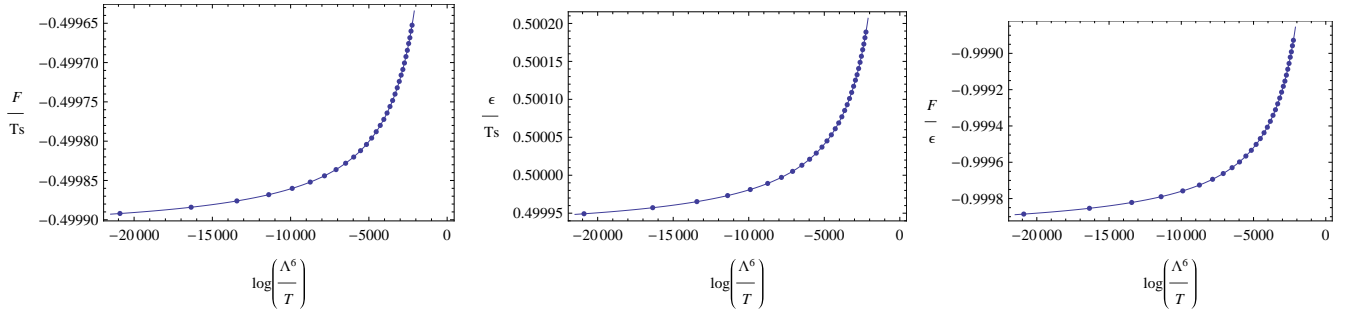


(c) Plots of \mathcal{F}/Ts , \mathcal{E}/Ts , and \mathcal{F}/\mathcal{E} , as a function of $\log(\Lambda^4/T)$ for $z = 4$. Dots are numerical results running h_0 from 2.2822 to 2.2816, which corresponds to $\log(\Lambda^4/T)$ from about -13000 to -1900. Solid line is fitting equations in table 1.

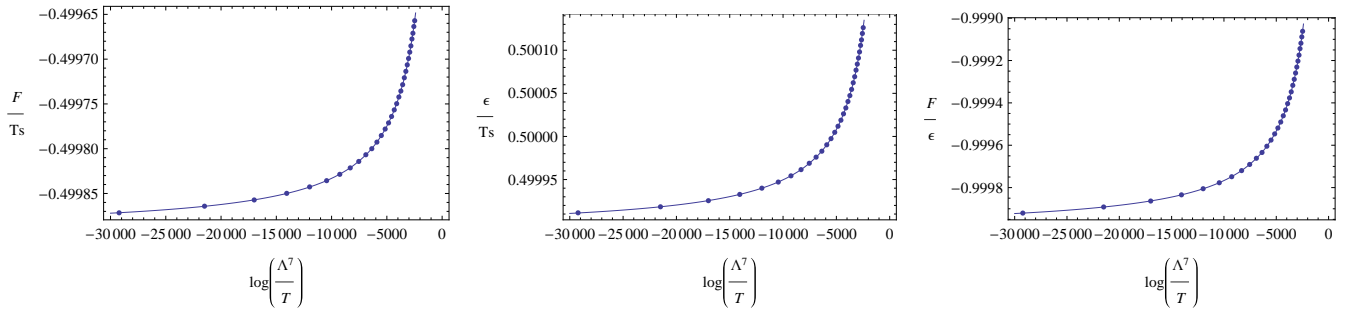
Figure 8: Plots of \mathcal{F}/Ts , \mathcal{E}/Ts and \mathcal{F}/\mathcal{E} versus $\log(\Lambda^z/T)$ for $z = 2, 3$, and 4.



(a) Plots of \mathcal{F}/Ts , \mathcal{E}/Ts , and \mathcal{F}/\mathcal{E} , as a function of $\log(\Lambda^5/T)$ for $z=5$. Dots are numerical results running h_0 from 2.9255 to 2.9249, which corresponds to $\log(\Lambda^5/T)$ from about -14000 to -2000. Solid line is fitting equations in table 1.

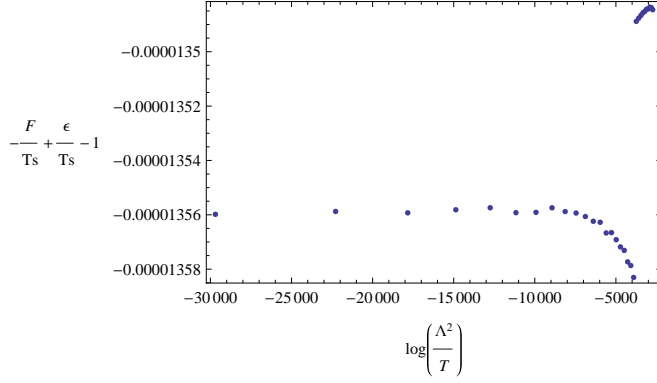


(b) Plots of \mathcal{F}/Ts , \mathcal{E}/Ts , and \mathcal{F}/\mathcal{E} , as a function of $\log(\Lambda^6/T)$ for $z=6$. Dots are numerical results running h_0 from 3.5668 to 3.5662, which corresponds to $\log(\Lambda^6/T)$ from about -21000 to -2200. Solid line is fitting equations in table 1.

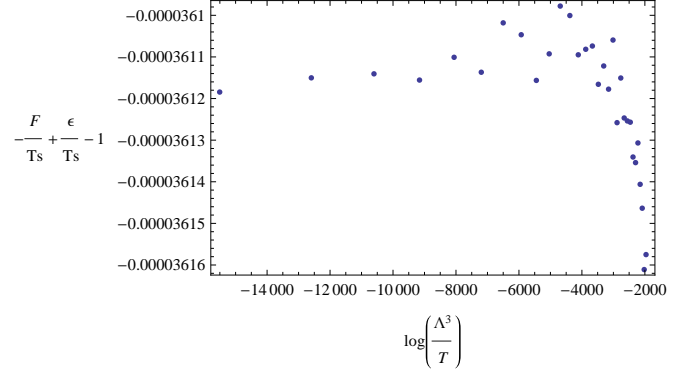


(c) Plots of \mathcal{F}/Ts , \mathcal{E}/Ts , and \mathcal{F}/\mathcal{E} , as a function of $\log(\Lambda^7/T)$ for $z=7$. Dots are numerical results running h_0 from 4.2070 to 4.2064, which corresponds to $\log(\Lambda^7/T)$ from about -30000 to -2200. Solid line is fitting equations in table 1.

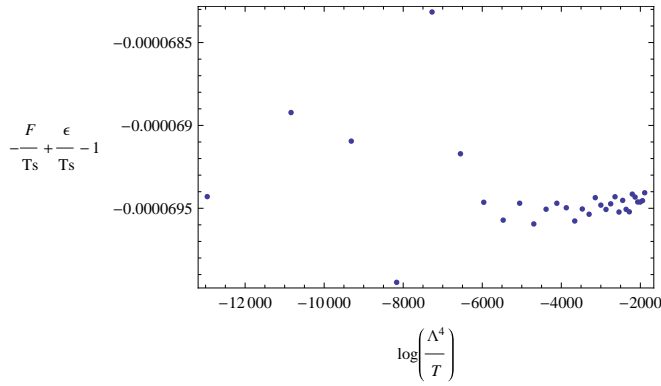
Figure 9: Plots of \mathcal{F}/Ts , \mathcal{E}/Ts and \mathcal{F}/\mathcal{E} versus $\log(\Lambda^z/T)$ for $z=5, 6$, and 7 .



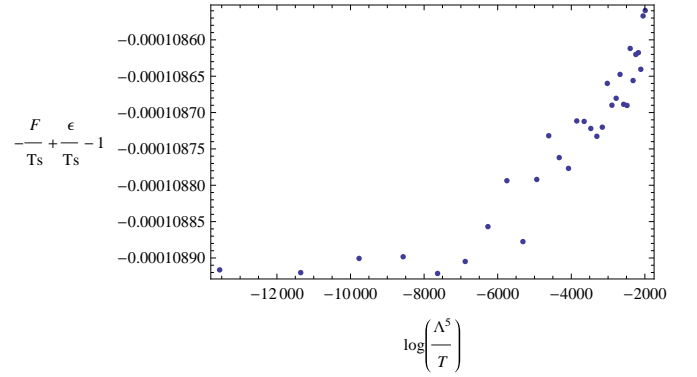
(a) Plots of $-\mathcal{F}/Ts + \mathcal{E}/Ts - 1$ for $z = 2$ and h_0 from 0.9713 to 0.9707.



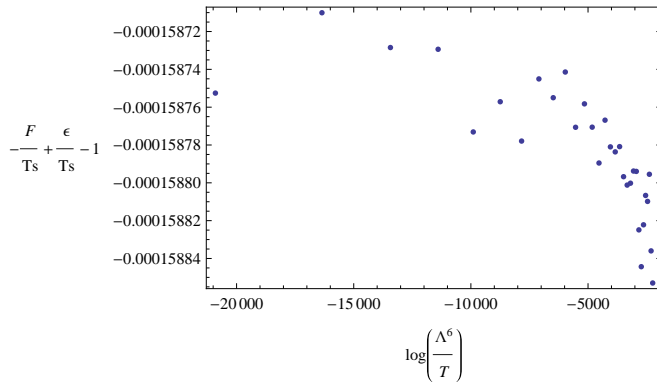
(b) Plots of $-\mathcal{F}/Ts + \mathcal{E}/Ts - 1$ for $z = 3$ and h_0 from 1.6343 to 1.6337.



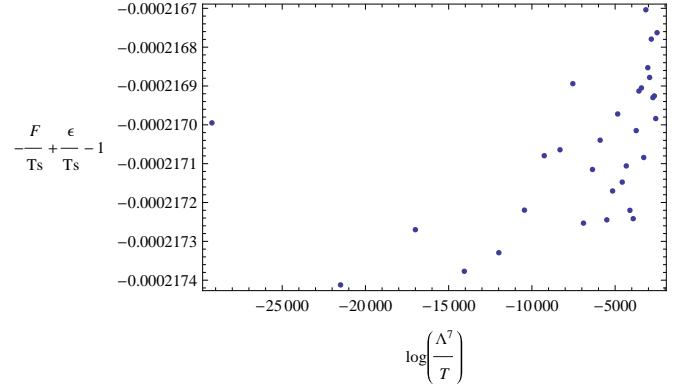
(c) Plots of $-\mathcal{F}/Ts + \mathcal{E}/Ts - 1$ for $z = 4$ and h_0 from 2.2822 to 2.2816.



(d) Plots of $-\mathcal{F}/Ts + \mathcal{E}/Ts - 1$ for $z = 5$ and h_0 from 2.9255 to 2.9249.



(e) Plots of $-\mathcal{F}/Ts + \mathcal{E}/Ts - 1$ for $z = 6$ and h_0 from 3.5668 to 3.5662.



(f) Plots of $-\mathcal{F}/Ts + \mathcal{E}/Ts - 1$ for $z = 7$ and h_0 from 4.2070 to 4.2064.

Figure 10: Entropy density over T versus $\log(\Lambda^z/T)$

Our results indicate that the basic physics of Lifshitz/QCT duality [6] is valid in higher dimensions. Regardless of dimensionality, with a small flux h_0 , renormalization group flow under the marginally relevant operators for UV-Lifshitz to IR-AdS was obtained in the zero temperature limit $\Lambda^z/T \rightarrow \infty$, commensurate with the 4-dimensional case [4]. This implies that we can expect RG flow to exist for each horizon flux, ranging from the zero temperature limit to asymptotically Lifshitz black hole spacetimes. The thermodynamic quantities, s/T , \mathcal{F}/Ts and \mathcal{E}/Ts were calculated as functions of $\log(\Lambda^z/T)$ just below the maximum value of h_0 (which describes a very slightly deformed Lifshitz space-time) and showed graphically similar behaviour. Also, as analytically expected, the leading-order terms from \mathcal{F}/Ts and \mathcal{E}/Ts from the first law of black hole thermodynamics for $\Lambda = 0$ can be numerically obtained. We also found the sub-leading terms in terms of $\log(\Lambda^z/T)$ when $\Lambda \sim 0$. This illustrates how physical quantities change as functions of $\log(\Lambda^z)/T$ upon approaching the critical point from a given phase. From a holographic duality perspective we can characterize the strongly coupled physics having the marginally relevant mode.

Since we considered the case for which the energy-momentum tensor of the gravitational field and the operator of the vector field become marginally relevant, we set $z = n - 1$. We consequently found that higher dimensional Lifshitz black holes can hold more flux, since the maximum value of h_0 increased with increasing n . The sub-leading term caused by the marginally relevant modes on the \mathcal{F}/Ts and \mathcal{E}/Ts has a weaker dependence on temperature T as dimensionality increases, as shown in table 2.

There are several possible directions for further research. One involves studying the relationship between the RG flows described here and previously noted stability issues in asymptotically Lifshitz space times [17]. Another involves consideration of marginally relevant modes in Lifshitz spacetimes with higher curvature corrections. The action with a Gauss-Bonnet term is now in progress [18].

Acknowledgements

This work was supported by the Natural Science and Engineering Research Council of Canada.

References

- [1] Juan Martin Maldacena, "The Large N limit of superconformal field theories and supergravity.", Adv. Theor. Math. Phys. **2**, (1998) 231-252, arXiv:hep-th/9711200.
- [2] D.T. Son, "Toward an AdS/cold atoms correspondence: a geometric realization of the Schrodinger symmetry", phys. Rev. D **78:046003**, arXiv:0804.3972 [hep-th].
- [3] S.S. Gubser, and J. McGreevy, "The gravity dual of a p -wave superconductor", JHEP, 0811:033, (2008), arXiv:0805.2960 [hep-th].
- [4] S. Kachru, X. Liu, and M. Mulligan, "Gravity duals of lifshitz-like fixed points.", Phys. Rev. D **78:106005**, (2008), arXiv:0808.1725 [hep-th].
- [5] M. H. Dehghani, and R. B. Mann, "Lovelock-Lifshitz Black Holes", JHEP, 1007:019, (2010), arXiv:1004.4397 [hep-th].
- [6] Miranda C.N. Cheng, Sean A. Hartnoll, and Cynthia A. Keeler, "Deformations of Lifshitz holography.", JHEP, 1003:062, (2010), arXiv:0912.2784 [hep-th].
- [7] S. F. Ross and O. Saremi, "Holographic stress tensor for non-relativistic theories", JHEP **0909**, 009 (2009) arXiv:0907.1846 [hep-th].

- [8] K. Balasubramanian and J. McGreevy, "*An analytic lifshitz black hole*", Phys. Rev. D **80:104039**, (2009), arXiv:0909.0263 [hep-th].
- [9] R. B. Mann and R. McNees, "*Holographic Renormalization for Asymptotically Lifshitz Spacetimes*", JHEP **1110**, 129 (2011) arXiv:1107.5792 [hep-th].
- [10] S. F. Ross, "*Holography for asymptotically locally Lifshitz spacetimes*", Class. Quant. Grav. **28**, 215019 (2011) arXiv:1107.4451 [hep-th].
- [11] S. Hollands, A. Ishibashi, and D. Marolf, "*Counter-term charges generate bulk symmetries*", Phys. Rev. D **72:104025**, (2005), arXiv:hep-th/0503105
- [12] M. Taylor, "*Non-relativistic holography*", arXiv:0812.0530 [hep-th]
- [13] Gaetano Bertoldi, Benjamin A. Burrington, and Amanda Peet, "*Black Holes in asymptotically Lifshitz spacetimes with arbitrary critical exponent.*", Phys. Rev. D **80:126003**, (2009), arXiv:0905.3183 [hep-th]
- [14] Robert B. Mann, "*Lifshitz Topological Black Holes.*", JHEP, 0906:075, (2009) arXiv:0905.1136 [hep-th]
- [15] U. H. Danielsson and L. Thorlacius, "*Black holes in asymptotically Lifshitz spacetime.*", JHEP, 0903:070, (2009) arXiv:0812.5088 [hep-th]
- [16] Gaetano Bertoldi, Benjamin A. Burrington, and Amanda W. Peet, "*Thermodynamics of black branes in asymptotically Lifshitz spacetimes.*", Phys. Rev. D **80:126004**, (2009), arXiv:0907.4755 [hep-th]
- [17] K. Copsey and R. Mann, "Pathologies in Asymptotically Lifshitz Spacetimes," JHEP **1103**, 039 (2011) [arXiv:1011.3502 [hep-th]].
- [18] Miok Park, and R. B. Mann, "*Generalization of Deformations of Lifshitz holography with Gauss-Bonnet term into $(n + 1)$ -dimensional spacetime*", in progress